AD-A073 203 AERONAUTICAL RESEARCH LABS MELBOURNE (AUSTRALIA) F/G 1/1
LATERAL AERODYNAMICS EXTRACTED FROM FLIGHT TESTS USING A PARAME--ETC(U)
OCT 78 R A FEIK

UNCLASSIFIED ARL/AERO NOTE-380 NL

1 OF 1
AD A073203

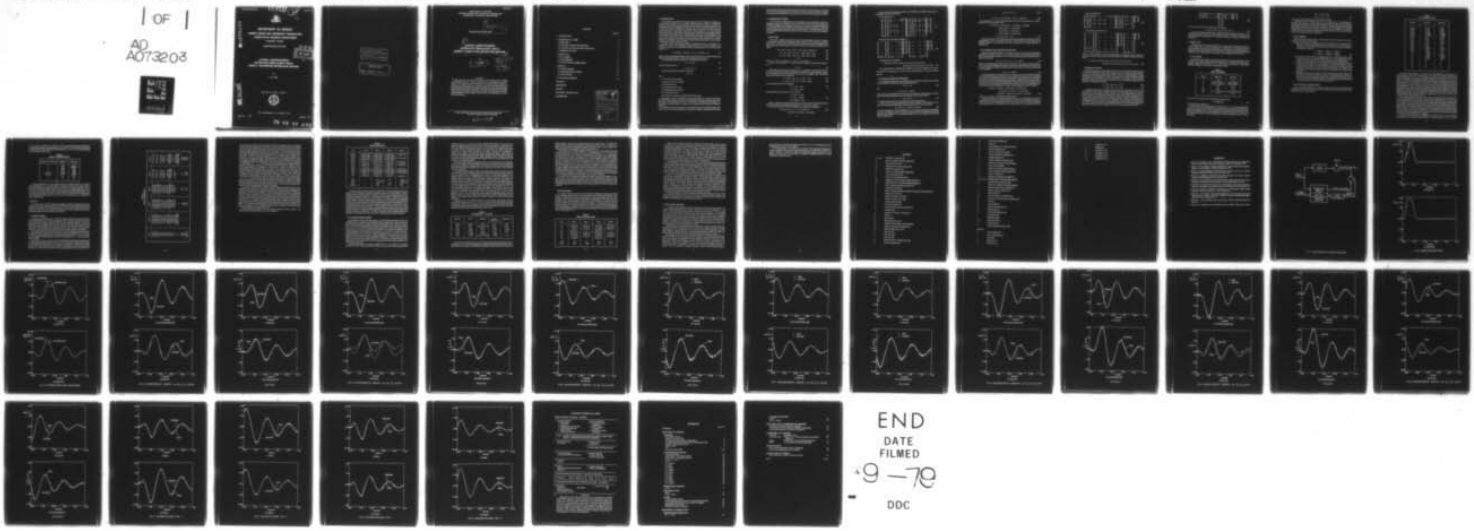

END
DATE FILMED
9-79
DDC

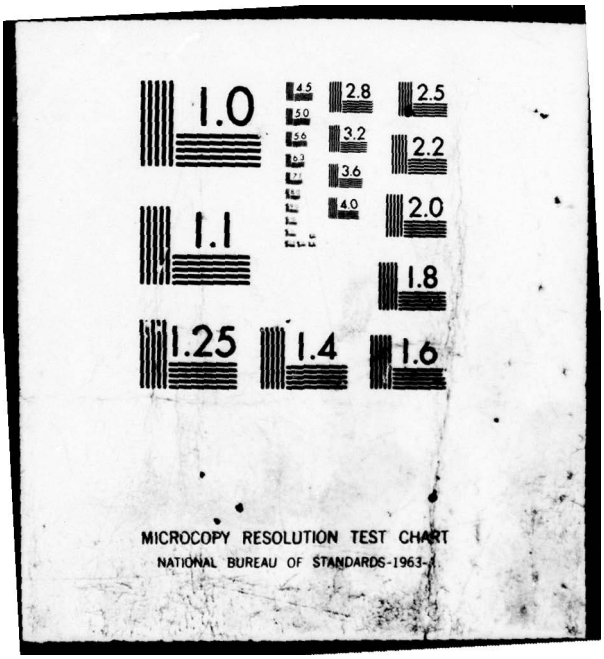
1.0
1.1
1.25
1.4
1.6
1.8
2.0
2.2
2.5
2.8
3.2
3.6
4.0
4.5
5.0
5.6
MICROCOPY RESOLUTION TEST CHART
NATIONAL BUREAU OF STANDARDS-1963-A

ARL-AERO-NOTE-380

LEVEL I 12

AR-001-311

DEPARTMENT OF DEFENCE

DEFENCE SCIENCE AND TECHNOLOGY ORGANISATION

AERONAUTICAL RESEARCH LABORATORIES

MELBOURNE, VICTORIA

AERODYNAMICS NOTE 380

LATERAL AERODYNAMICS EXTRACTED FROM FLIGHT TESTS USING A PARAMETER ESTIMATION METHOD

by

R. A. FEIK

Approved For Public Release.

COPY No 18

OCTOBER, 1978

AR-001-311

DEPARTMENT OF DEFENCE
DEFENCE SCIENCE AND TECHNOLOGY ORGANISATION
AERONAUTICAL RESEARCH LABORATORIES

(14) ARL/AERO 7

AERODYNAMICS NOTE-380

(6)

LATERAL AERODYNAMICS EXTRACTED FROM FLIGHT TESTS USING A PARAMETER ESTIMATION METHOD

by

(10) R. A. FEIK

(11) Oct 78

(12) 48p.

SUMMARY

Flight data from a 60° delta wing aircraft have been analysed using a modified Newton-Raphson parameter estimation procedure. The model equations used for the analysis were extended to account for sideslip vane errors and for lateral accelerometer position error. Lateral derivatives extracted from the data have been compared with wind tunnel measurements and theoretical estimates and areas of agreement and disagreement identified. The method has also been applied to the analysis of fin loads measured in flight and some tentative conclusions reached. The results confirm the effectiveness of the parameter identification procedure in flight test analysis and its ready applicability to a variety of related problems.

POSTAL ADDRESS: Chief Superintendent, Aeronautical Research Laboratories,
Box 4331, P.O., Melbourne, Victoria, 3001, Australia.

CONTENTS

1. INTRODUCTION

The modified Newton-Raphson parameter estimation method described in References 1 and 2 has been adapted for use on the ARL PDP10 computer. In support of mathematical modelling activities being presently undertaken the method provides a means for systematic and rational validation of a mathematical model as well as a means of obtaining aerodynamic data not otherwise available. In Reference 3 a detailed study of the method was made to establish requirements, such as input design, sampling rates, record length, etc., for a successful application of the method to the analysis of response records. The method was subsequently applied[4] to the analysis of actual flight test data of the longitudinal response of a delta wing fighter aircraft to elevator inputs. The present study, looking at the lateral response of the aircraft to rudder inputs, raises a number of new aspects which complement the work of Reference 4. In addition the analysis is extended to the estimation of airload parameters which govern the forces experienced by the fin when the aircraft is in flight.

The basic concept of the estimation method is summarised in Figure 1. The objective is to determine that value of the mathematical model parameter vector, $\mathbf{c}$, which minimises a cost functional, J, proportional to the difference between the measured response, $\mathbf{z}$, and the calculated response, $\mathbf{y}$, i.e.

$$J = (1/N) \sum_{i=1}^{N} (\mathbf{z}_i - \mathbf{y}_i)^T D_1 (\mathbf{z}_i - \mathbf{y}_i) + (\mathbf{c} - \mathbf{c}_o)^T D_2 (\mathbf{c} - \mathbf{c}_o) \tag{1}$$

where D_1 and D_2 are diagonal weighting matrices and the second term is a weighted mean square difference between the parameter vector $\mathbf{c}$ and a stipulated *a priori* value, $\mathbf{c}_o$.

The mathematical model is described by a state equation of the form

$$\dot{\mathbf{x}} = A\mathbf{x} + B\mathbf{u} \tag{2}$$

and the calculated response is

$$\mathbf{y} = F\mathbf{x} + G\mathbf{u} + \mathbf{b}. \tag{3}$$

The measured response is assumed to be given by

$$\mathbf{z} = \mathbf{y} + \mathbf{n} \tag{4}$$

where

$\mathbf{x}$ is the vector of state variables,

$\mathbf{u}$ is the vector of control variables,

$\mathbf{y}$ is the response vector,

$\mathbf{b}$ is a measurement bias vector,

$\mathbf{z}$ is the measured response vector,

$\mathbf{u}$ is a random noise vector,

A, B, F and G are matrices of parameters defining the model.

The parameter vector, $\mathbf{c}$, contains some or all of the elements of A, B, F and G, the elements of $\mathbf{b}$ and the initial conditions. The iterative modified Newton-Raphson procedure is used to find that value of $\mathbf{c}$ which minimises the cost, J. An indication of the quality of the estimates, $\mathbf{c}$, is given by the Cramer-Rao bound, σ_{CR}, which is a lower bound on the variance of the estimates (see Ref. 2).

The detailed form of the model equations is developed in Section 2 and includes allowance for sideslip vane errors and lateral accelerometer corrections. In addition, equations for the fin loads

are also outlined. Section 3 describes the flight data, pre-analysis data conditioning, and discusses the *a priori* values and weights used in the analysis. Results are presented in Section 4, together with discussion and comparison with theoretical values of several of the aerodynamic derivatives.

2. MATHEMATICAL MODEL

In this section the detailed form of the mathematical model, described in general by Equations (1) and (2), is developed. Firstly, the basic linear small perturbation equations for aircraft lateral response to control input are outlined. Next an extension of the model is developed in order to deal with errors in sideslip vane measurements and this is followed by a method for incorporating lateral accelerometer corrections into the model for a case where these corrections cannot be directly made to the measurements. Finally a model for obtaining fin load parameters is described.

2.1 Basic Model

The aircraft is assumed to be initially trimmed in steady level flight at speed V_e, incidence α_e and attitude θ_e. Lateral small disturbance motions about this trim state can be produced by either aileron or rudder inputs. The linearised equations describing the small disturbance lateral motions following a control input can be written, in body axes, as follows (see Reference 5 for details):

$$m\dot{v} = Y_\beta\beta + Y_{\delta_r}\delta r + Y_{\delta_a}\delta a - mu_e r + mw_e p + mg\cos\theta_e \,.\, \phi \tag{5a}$$

$$I_x\dot{p} - I_{xz}\dot{r} = L_\beta\beta + L_p p + L_r r + L_{\dot\beta}\dot\beta + L_{\delta_r}\delta r + L_{\delta_a}\delta a \tag{5b}$$

$$I_z\dot{r} - I_{xz}\dot{p} = N_\beta\beta + N_p p + N_r r + N_{\dot\beta}\dot\beta + N_{\delta_r}\delta r + N_{\delta_a}\delta a \tag{5c}$$

$$\dot\phi = p \tag{5d}$$

where $w_e = V_e \sin\alpha_e \approx V_e\alpha_e$ and $u_e = V_e\cos\alpha_e \simeq V_e$ for small α_e.

Further, from the definition $v = V\sin\beta$ it follows, for constant speed and small sideslip, β, that

$$\dot v = V_e\dot\beta. \tag{6}$$

Hence Equation (5a) becomes an equation for $\dot\beta$ by substitution of Equation (6). This can then be used to eliminate the $\dot\beta$ terms from Equations (5b) and (5c). In the present case, however, this is not necessary since it can be assumed that $L_{\dot\beta}$ and $N_{\dot\beta}$ are negligible. After some algebra, Equations (5b) and (5c) can be rewritten as

$$\dot p = L'_\beta\beta + L'_p p + L'_r r + L'_{\delta_r}\delta r + L'_{\delta_a}\delta a \tag{7a}$$

$$\dot r = N'_\beta\beta + N'_p p + N'_r r + N'_{\delta_r}\delta r + N'_{\delta_a}\delta a \tag{7b}$$

where the dashed derivatives are defined as

$$\begin{aligned} L'_c &= I'_{xz}N_c + L_c/I'_x \\ N'_c &= I'_{xz}L_c + N_c/I'_z \end{aligned} \tag{8}$$

with the subscript c standing for β, p, r, δ_r or δ_a and

$$\begin{aligned} I'_x &= (I_xI_z - I^2_{xz})/I_z \\ I'_z &= (I_xI_z - I^2_{xz})/I_x \\ I'_{xz} &= I_{xz}/(I_xI_z - I^2_{xz}). \end{aligned} \tag{9}$$

Since I_{xz} is small in the present case and can be assumed to be zero the relations given by Equations (8) and (9) are considerably simplified, e.g. $L'_c = L_c/I_x$, $N'_c = N_c/I_z$.

Finally, the equation for the lateral acceleration, n_y, follows from the definition

$$\begin{aligned} (g/V_e)n_y &= (\dot v + u_e r - w_e p - g\cos\theta_e \,.\, \phi)/V_e \\ &\simeq (Y_\beta/mV_e)\beta + (Y_{\delta_r}/mV_e)\delta_r + (Y_{\delta_a}/mV_e)\delta_a. \end{aligned} \tag{10}$$

Thus the basic mathematical model used for the analysis of the lateral motion may be summarised in matrix form as follows.

The state equations are:

$$\begin{bmatrix} \dot{\beta} \\ \dot{p} \\ \dot{r} \\ \dot{\phi} \end{bmatrix} = \begin{bmatrix} \frac{Y_\beta}{mV_e} & \alpha_e & -1 & \frac{g\cos\theta_e}{V_e} \\ \frac{L_\beta}{I_x} & \frac{L_p}{I_x} & \frac{L_r}{I_x} & 0 \\ \frac{N_\beta}{I_z} & \frac{N_p}{I_z} & \frac{N_r}{I_z} & 0 \\ 0 & 1 & 0 & 0 \end{bmatrix} \begin{bmatrix} \beta \\ p \\ r \\ \phi \end{bmatrix} + \begin{bmatrix} \frac{Y_{\delta r}}{mV_e} & \frac{Y_{\delta a}}{mV_e} & Y_o \\ \frac{L_{\delta r}}{I_x} & \frac{L_{\delta a}}{I_x} & L_o \\ \frac{N_{\delta r}}{I_z} & \frac{N_{\delta a}}{I_z} & N_o \\ 0 & 0 & 0 \end{bmatrix} \begin{bmatrix} \delta_r \\ \delta_a \\ 1 \end{bmatrix} \tag{11}$$

The equations for the response variables are:

$$\begin{bmatrix} \beta \\ p \\ r \\ \phi \\ n_y(g/V_e) \end{bmatrix} = \begin{bmatrix} 1 & 0 & 0 & 0 \\ 0 & 1 & 0 & 0 \\ 0 & 0 & 1 & 0 \\ 0 & 0 & 0 & 1 \\ Y_\beta/mV_e & 0 & 0 & 0 \end{bmatrix} \begin{bmatrix} \beta \\ p \\ r \\ \phi \end{bmatrix} + \begin{bmatrix} 0 & 0 & 0 \\ 0 & 0 & 0 \\ 0 & 0 & 0 \\ 0 & 0 & 0 \\ Y_{\delta r}/mV_e & Y_{\delta a}/mV_e & Y_o \end{bmatrix} \begin{bmatrix} \delta_r \\ \delta_a \\ 1 \end{bmatrix} \tag{12}$$

The parameter vector is given by:

$$\mathbf{c} = [Y_\beta/mV_e,\ Y_{\delta r}/mV_e,\ Y_{\delta a}/mV_e,\ L_\beta/I_x,\ L_p/I_x,\ L_r/I_x,\ L_{\delta r}/I_x,\ L_{\delta a}/I_x,$$
$$N_\beta/I_z,\ N_p/I_z,\ N_r/I_z,\ N_{\delta r}/I_z,\ N_{\delta a}/I_z,\ Y_o,\ L_o,\ N_o,]^T \tag{13}$$

The measurement bias, **b** (appearing in Equation (3)), has been neglected in the above equations and the parameters Y_o, L_o, and N_o have been introduced to account for possible state bias.

2.2 Corrections to Sideslip Vane Measurements

The sideslip measurements, β_m, are influenced by yaw and roll rate effects, and are related to the true sideslip, β, by the following equations (Reference 5):

$$\beta_m = \beta - \beta_s \tag{14}$$

with

$$\beta_s = p(z_v/V_e) - r(x_v/V_e)$$

where x_v and z_v are the distances of the vane forward and below the centre of gravity. In order to account for possible calibration slope errors, Equation (14) has been modified to

$$\beta_m = G\beta - \beta_s \tag{15}$$

with G becoming a parameter to be identified during the matching process.

Since the vane was not dynamically balanced, it also responds to accelerations.[6] The correction to the measured sideslip due to lateral acceleration at the vane can be written:

$$\beta_d = K(\dot{r}(x_v/V_e) - \dot{p}(z_v/V_e) + n_y(g/V_e)) \tag{16}$$

where yaw acceleration, $\dot{r}$, and roll acceleration, $\dot{p}$, are in radians/sec^2 and lateral acceleration, n_y, is in g's. An estimated value for the constant of proportionality, K, depending on vane characteristics, is given in Section 3.1. The measured sideslip, β_m, can now be related to the true sideslip, β, by the equation

$$\beta_m = G\beta - \beta_s + \beta_d \tag{17}$$

or

$$\beta_m + \beta_s = G\beta + K(\dot{r}(x_v/V_e) - \dot{p}(z_v/V_e) + n_y(g/V_e)). \tag{18}$$

By substituting for $\dot{r}$, $\dot{p}$, and n_y from Equations (7) and (10), and assuming δ_a to be zero, Equation (18) can be expanded to give:

$$\begin{aligned}\beta_m + \beta_s &= [G + K[(x_v/V_e)N_\beta/I_z - (z_v/V_e)L_\beta/I_x + Y_\beta/mV_e]]\beta \\ &\quad + K[(x_v/V_e)N_p/I_z - (z_v/V_e)L_p/I_x]p \\ &\quad + K[(x_v/V_e)N_r/I_z - (z_v/V_e)L_r/I_x]r \\ &\quad + K[(x_v/V_e)N_{\delta r}/I_z - (z_v/V_e)L_{\delta r}/I_x]\delta_r \\ &= a_1\beta + a_2 p + a_3 r + b_1\delta_r \end{aligned} \tag{19}$$

The corrections due to roll and yaw rates, β_s, are readily calculated from Equation (14) since measurements of p and r are available. Thus $(\beta_m + \beta_s)$ rather than β_m can be treated as the response variable to be matched with the model results given by the right hand side of Equation (19).

2.3 Corrections to Lateral Accelerometer Measurements

Since the lateral accelerometer is not located at the centre of gravity the acceleration measured by it will differ from the value at the centre of gravity. If the accelerometer position is given by the body axes co-ordinates (x_a, y_a, z_a) then the relation between the measured and c.g. values can be written[5]:

$$n_{y_m} = n_y + (x_a\dot{r} - z_a\dot{p} - y_a r^2 - y_a p^2)/g \tag{20}$$

where n_{y_m} is the measured acceleration and n_y is the value at the c.g. The dominant correction term in the present investigation was found to be that due to roll acceleration, $\dot{p}$, caused by the location of the lateral accelerometer approximately 0·6 m (2 ft) below the c.g. Hence Equation (20) can be simplified to

$$n_{y_m} = n_y - (z_a/g)\dot{p}. \tag{21}$$

If measurements of $\dot{p}$ were available then the correction $(z_a/g)\dot{p}$ could immediately be applied to the measured acceleration. However, as $\dot{p}$ is not available in the present case one possibility is to proceed with the identification without correcting and, using the value of $\dot{p}$ thus calculated, then make the correction and repeat the matching process. Another alternative, adopted here, is to allow for the correction within the mathematical model itself by calculating the right hand side of Equation (21) and matching this directly with the measured value, n_{y_m}. Substituting for n_y and $\dot{p}$ in Equation (21) from Equations (7) and (10), and assuming δ_a to be zero, results in

$$\begin{aligned}(g/V_e)n_{y_m} &= [Y_\beta/mV_e - (z_a/V_e)L_\beta/I_x]\beta - (z_a/V_e)(L_p/I_x)p \\ &\quad - (z_a/V_e)(L_r/I_x)r + [Y_{\delta r}/mV_e - (z_a/V_e)L_{\delta r}/I_x]\delta_r \\ &= (y_\beta/mV_e)\beta + (y_p/mV_e)p + (y_r/mV_e)r + (y_{\delta r}/mV_e)\delta_r \end{aligned} \tag{22}$$

where y_β, y_p, y_r and $y_{\delta r}$ are modified side force derivatives.

Thus Equation (22), for n_{y_m}, replaces Equation (10), for n_y, in the mathematical model. The full equations, including the corrections outlined in this section and the sideslip corrections of Section 2.2 may now be summarised. Since there was no aileron input in the course of the flight tests the equations have been simplified by removing the aileron, δ_a, term from the input vector.

The state equations are:

$$\begin{bmatrix} \dot{\beta} \\ \dot{p} \\ \dot{r} \\ \dot{\phi} \end{bmatrix} = \begin{bmatrix} Y_\beta/mV_e & \alpha_e & -1 & g\cos\theta_e/V_e \\ L_\beta/I_x & L_p/I_x & L_r/I_x & 0 \\ N_\beta/I_z & N_p/I_z & N_r/I_z & 0 \\ 0 & 1 & 0 & 0 \end{bmatrix} \begin{bmatrix} \beta \\ p \\ r \\ \phi \end{bmatrix} + \begin{bmatrix} Y_{\delta_r}/mV_e & Y_o \\ L_{\delta_r}/I_x & L_o \\ N_{\delta_r}/I_z & N_o \\ 0 & 0 \end{bmatrix} \begin{bmatrix} \delta_r \\ 1 \end{bmatrix} \tag{23}$$

The response equations become:

$$\begin{bmatrix} \beta \\ p \\ r \\ \phi \\ (\beta_m+\beta_s) \\ (g/V_e)n_{y_m} \end{bmatrix} = \begin{bmatrix} 1 & 0 & 0 & 0 \\ 0 & 1 & 0 & 0 \\ 0 & 0 & 1 & 0 \\ 0 & 0 & 0 & 1 \\ a_1 & a_2 & a_3 & 0 \\ y_\beta/mV_e & y_p/mV_e & y_r/mV_e & 0 \end{bmatrix} \begin{bmatrix} \beta \\ p \\ r \\ \phi \end{bmatrix} + \begin{bmatrix} 0 & 0 \\ 0 & 0 \\ 0 & 0 \\ 0 & 0 \\ b_1 & b_o \\ y_{\delta_r}/mV_e & y_o \end{bmatrix} \begin{bmatrix} \delta_r \\ 1 \end{bmatrix} \tag{24}$$

where b_o, y_o are introduced to account for possible bias. The parameter vector, excluding b_1, y_p/mV_e and y_r/mV_e, which were held constant throughout as discussed in Section 3.3, can be written

$$\mathbf{c} = [Y_\beta/mV_e,\ Y_{\delta_r}/mV_e,\ y_\beta/mV_e,\ y_{\delta_r}/mV_e,\ L_\beta/I_x,\ L_p/I_x,\ L_r/I_x,\ L_{\delta_r}/I_x,$$
$$N_\beta/I_z,\ N_p/I_z,\ N_r/I_z,\ N_{\delta_r}/I_z,\ a_1,\ a_2,\ a_3,\ Y_o,\ L_o,\ N_o,\ b_o,\ y_o]^T \tag{25}$$

2.4 Equations for Fin Loads

While the response vector, Equation (24) in Section 2.3, consists of elements usually measured in the course of stability and control flight testing, the method of analysis does not place any restrictions on the elements making up the response vector. For example, Reference 7 applies the method to the determination of in-flight airload parameters. During the flight tests under consideration here, strain gauges in the fin measured Shear, S, and Tension, T, forces. Following Reference 7, these forces can be related to the state and control variables through the following linearised small disturbance equations:

$$S = S_\beta\beta + S_p p + S_r r + S_{\delta_r}\delta r \tag{26}$$

$$T = T_\beta\beta + T_p p + T_r r + T_{\delta_r}\delta r \tag{27}$$

In Equations (26) and (27) the inertial and/or gravitational contributions to S and T have been neglected as being small. To identify the Shear and Tension parameters (S_β, T_β, etc.) the response vector can be readily extended to include S and T as additional elements so that the S and T records may be matched simultaneously with the other records. Alternatively, a two part procedure can be followed since the airload parameters of Equations (26) and (27) are completely uncoupled from the other aircraft parameters. The first step would identify the aircraft parameters as usual and these would subsequently be held constant. In the second stage only S and T would be matched. The mathematical model for the second stage would have the same state equations as given by Equation (23) while the response equations would be:

$$\begin{bmatrix} S \\ T \end{bmatrix} = \begin{bmatrix} S_\beta & S_p & S_r & 0 \\ T_\beta & T_p & T_r & 0 \end{bmatrix} \begin{bmatrix} \beta \\ p \\ r \\ \phi \end{bmatrix} + \begin{bmatrix} S_{\delta r} & S_o \\ T_{\delta r} & T_o \end{bmatrix} \begin{bmatrix} \delta_r \\ 1 \end{bmatrix} \tag{28}$$

where S_o, T_o are bias terms. The parameter vector becomes

$$\mathbf{c} = [S_\beta, S_p, S_r, S_{\delta r}, T_\beta, T_p, T_r, T_{\delta r}, S_o, T_o]^T \tag{29}$$

The second method has been used in obtaining the results described in Section 4.3. No significant change in the accuracy of the parameters is expected compared to the method which treats all equations simultaneously, but a significant reduction in computer time results (see Reference 7).

3. FLIGHT DATA

The flight data to be analysed is discussed in this section. The test conditions and the form of the available data is first outlined followed by a description of the corrections and pre-processing applied to the basic data in preparation for the Modified Newton-Raphson program. Finally the *a priori* values used for each of the parameters of interest is summarised followed by a discussion of the values chosen for the elements of the weighting matrices D_1 and D_2.

3.1 Test Conditions

The flight test data consisted of time response records of a 60° delta wing fighter aircraft following a pilot applied rudder pulse input. Records for two different Mach numbers were available, namely $M = 0{\cdot}96$ and $M = 0{\cdot}72$. The relevant test conditions for these flights, referred to as flights RK1 and RK2 are summarised in Table 1.

TABLE 1
Flight Test Conditions

Details	Flight RK1	Flight RK2
M	0·96	0·72
h	9076 m (29,770 ft)	2985 m (9791 ft)
V_e	292·4 m/s (568 kt)	236 m/s (459 kt)
α_e	3·73°	2·71°
θ_e	2·87°	3·12°
$(\delta_e)_e$	−0·78°	−0·61°
c.g.	50·33% of ℄ chord	48·95% of ℄ chord
K	0·293	0·237

The values of K given in Table 1 were estimated using the formula

$$K = 0{\cdot}00984\, V_e/g \tag{30}$$

which was derived in Reference 4.

Measured data consisted of response time histories of β, p, r, n_y, and δ_r. Approximately 15 seconds of record was available but only 5 seconds were used in any single analysis. This represented approximately 2 to 3 cycles of oscillation. The data rate was 60 samples/sec and from inspection of the flight records it was determined that the natural frequency, ω_n, was about 3·2 rad/s for flight RK1 and 3·7 rad/s for flight RK2. Assuming an in-between value of 3·5 rad/s this implies

$$\omega_n \Delta t = 3 \cdot 5/60 = 0 \cdot 06$$

$$\omega_n T = 3 \cdot 5 \times 5 = 17 \cdot 5 \tag{31}$$

where Δt is the sampling interval and T the total record length.

In Reference 3 it was found that values of $\omega_n \Delta t < 0 \cdot 14$ and $\omega_n T > 14$ were adequate for matching of the response to a rudder doublet input. Although in the present case the input is a pulse rather than a doublet, the values given in Equation (31) suggest that the sampling rate and record length should be ample for successful matching. In fact no difficulties of convergence or identification were encountered. Normally seven iterations were specified in the program, though it was found that good convergence was invariably achieved by the fourth or fifth iteration with only small improvements subsequently.

3.2 Data Conditions

Before proceeding with the analysis a certain amount of pre-processing of the data was performed. This included the following—

(*a*) Roll and yaw rate gyro misalignment corrections according to the equations given in Reference 5. Using the gyro alignment data the corrected roll rate, p, and yaw rate, r, are obtained from the measured roll, pitch and yaw rates, p_m, q_m and r_m respectively, according to the equations

$$p = 0 \cdot 9996 p_m + 0 \cdot 00131 q_m - 0 \cdot 0291 r_m$$

$$r = 0 \cdot 0278 p_m - 0 \cdot 0452 q_m + 1 \cdot 00092 r_m \tag{32}$$

(*b*) Corrections to angle of sideslip measurements due to yaw and roll rate effects as discussed in Section 2.2. The corrected sideslip angle, $\beta_m + \beta_s$, was subsequently matched where β_m is the measured value and β_s is the correction given by Equation (14).

(*c*) A smooth curve was hand fitted to the rudder input data as shown in Figures 2*a* and 2*b*. Although this smoothing is not strictly necessary it was thought desirable to remove the obvious spikes caused by a noisy transducer (see Figure 2*a* in particular) since the identification method makes no allowance for noise in the input. For a relatively noise free record, such as that in Figure 2*b*, the effect of smoothing on the results is hardly discernible.

(*d*) Because the roll rate gyro saturated at a fairly low level, the initial peak of the roll rate record was cut off as shown in Figures 3*a* and 3*b*. The missing portion was filled in by hand after choosing an appropriate peak level by comparison with the other records. The result is also shown in Figures 3*a* and 3*b*. The effect of this rather arbitrary procedure on the matched results will be discussed further in Section 4.

3.3 A Priori Values and Weighting Matrices

The *a priori* values assigned to the various parameters were mainly obtained from wind tunnel tests (e.g. Ref. 8) or else were estimated from data sheet sources. Table 2 summarises the values used in the two cases analysed.

TABLE 2
A Priori Parameter Values

Parameter	Flight RK1	Flight RK2
Y_β/mV_e	−0·184	−0·292
$Y_{\delta r}/mV_e$	−0·026	−0·040
y_β/mV_e	−0·120	−0·226
y_p/mV_e	0·00403	0·00465
y_r/mV_e	−0·00139	−0·00187
$y_{\delta r}/mV_e$	−0·015	−0·021
L_β/I_x	−30·67	−25·82
L_p/I_x	−1·92	−1·78
L_r/I_x	0·661	0·684
$L_{\delta r}/I_x$	−5·38	−7·57
N_β/I_z	12·06	17·44
N_p/I_z	−0·0066	0·0126
N_r/I_z	−0·594	−0·563
$N_{\delta r}/I_z$	4·007	5·79
a_1	1·0076	1·079
a_2	0·0012	0·0015
a_3	−0·0059	−0·0074
b_1	0·033	0·051
Y_o	0	0
y_o	0	0
L_o	0	0
N_o	0	0
b_o	0	0

The yawing moment derivatives, N_β and $N_{\delta r}$, have been adjusted to the correct centre of gravity position for each flight. The derivatives y_β, y_p, y_r, and $y_{\delta r}$ are defined by Equation (22) while the parameters a_1, a_2, a_3, and b_1 are defined by Equation (19). In both cases the *a priori* values were calculated from the respective definitions using $x_v = 9{\cdot}15$ m (30 ft), $z_v = 0{\cdot}6$ m (2 ft) and $z_a = 0{\cdot}6$ m (2 ft). For flight RK1 the values of the aerodynamic derivatives appearing in the definitions were set at their respective *a priori* values, as in Table 2. For flight RK2 on the other hand, an initial run was made with z_a, z_v and x_v all set to zero and the aerodynamic derivatives thus identified were used to evaluate the formulae of Equations (19) and (22). Several of the parameters listed in Table 2 are weak in the sense that they only slightly influence the calculated results and, conversely, the information available in the flight records is insufficient to alter them significantly from the *a priori* values assigned. This applies in particular to y_p, y_r and b_1, which were consequently held constant at their *a priori* values and also to a_2 and a_3 which were only allowed to vary in one case (see Section 4.1).

The weighting assigned to the *a priori* values of each of the parameters which were allowed to vary was established, as in Reference 4, by assuming a standard deviation, σ, equal to 20% of the parameter value. Then the relevant element of the weighting matrix D_2 becomes simply $1/\sigma^2$. The choice of 20% is not critical with only small differences in the identified results following from a value of 10%. In general the smaller the value of σ the more the identified parameter values, especially those of the weaker parameters, tend towards the *a priori* value. Those parameters in Table 2 with zero *a priori* values were assigned very small weighting thus allowing them freedom to take up whatever value they may tend towards, no matter how weakly. In addition, during the analysis of fin loads, all the parameters in Equation (29) describing the fin loads were assigned zero *a priori* values and effectively zero weighting.

The elements of D_1 determine the weighting to be assigned to each of the time histories being matched. In the present case these include, at one time or another, $\beta_m + \beta_s$, p, r, $(g/V_e)n_y$

as well as shear, S, and tension, T, records. In order to give approximately equal weighting to each matched time history a standard deviation, σ_m, equal to 5% of the maximum value of each measured record was selected and the relevant element of D_1 set to $1/\sigma^2_m$. The resulting weights are summarised in Table 3 below.

TABLE 3
Elements of Weighting Matrix D_1

Response vector element	Flight RK1	Flight RK2
β	0·001	0·001
p	816	3906 (657)
r	6400	3906
ϕ	0·001	0·001
$(\beta_m + \beta_s)$	51653	41649
$(g/V_e)n_y$	2777777	1041233
S	17·1	14·0
T	5·2	3·8

It should be noted that the final identified results do not depend critically on the weights. Thus for flight RK2 the same weight (3906) was assigned to both p and r records (Table 3) instead of assigning to p the more appropriate, according to the previous argument, value of 657. The only discernible difference thus produced was in the weighted mean square match error $s^2(p)$, as is to be expected. For records not being matched the corresponding element of D_1 can be set to a small value. This applies to β and ϕ in Table 3. In the case of ϕ no measurements were available for matching while in the case of β the corrected value, $\beta_m + \beta_s$, rather than β itself, is being matched.

4. RESULTS

In this section the results of the parameter estimation analysis of the flight manoeuvres are presented. The matches obtained between the mathematical model calculations and the flight records are first discussed. This is followed by a closer look at the values obtained for the various aerodynamic derivatives and a comparison with the *a priori* estimates and theoretical estimates. Finally, the results of the fin load analysis are presented.

4.1 Results of Matching

The results from flight RK1 at $M = 0{\cdot}96$ are presented in Figures 4–7 and in Table 4 below. Table 4 summarises the *a priori* values and respective weights in the first column with the results (plus Cramer-Rao bounds) of several identification runs in subsequent columns. Note that the parameters a_2 and a_3, though usually fixed, were allowed to vary in case RK1-4. As can be seen from Table 4, the identified values of a_2 and a_3 did not differ from their respective *a priori* estimates nor did the Cramer-Rao bounds differ from the *a priori* weights. It is clear then that a_2 and a_3 are weak parameters and holding them fixed in all other cases is not a restriction.

The rudder input in each case is the smoothed curve shown in Figure 2*a*. It should be pointed out that smoothing of the rudder input in the present case makes little difference to the results. In addition, the slight difference in the smoothed and measured record for $t > 1{\cdot}30$ sec in Figure 2*a* is not significant. Cases have been run with δ_r set to 0·004 rad. for $t > 1{\cdot}30$ sec with almost identical results.

In case RK1-1, shown in Figure 4, all the available flight records have been matched using the full mathematical model summarised in Section 2.3. The match is not as good as may be hoped for with fairly large mean square errors, s^2, as shown in column RK1-1 of Table 4. One possible cause for this may be inadvertent errors introduced by extrapolation of the p record as shown in Figure 3*a*. To check this possibility the match was repeated with the p record excluded. The

TABLE 4
Results from Flight RK1

Item	*A priori*	RK1-1	RK1-2	RK1-3	RK1-4
Y_β/mV_e	−0·184±0·037	−0·140±0·036	−0·162±0·036	−0·167±0·036	−0·165±0·036
$Y_{\delta r}/mV_e$	−0·026±0·005	−0·030±0·005	−0·028±0·005	—	—
y_β/mV_e	−0·120±0·024	−0·098±0·013	−0·107±0·015	−0·095±0·017	−0·090±0·016
$y_{\delta r}/mV_e$	−0·015±0·003	−0·0073±0·0029	−0·011±0·0029	—	—
L_β/I_x	−30·67±6·13	−23·89±2·78	−16·57±5·26	−21·83±5·67	−24·25±3·40
L_p/I_x	−1·92±0·38	−1·53±0·30	−1·95±0·37	−1·84±0·37	−1·69±0·33
L_r/I_x	0·661±0·13	0·653±0·13	0·654±0·13	0·651±0·13	0·651±0·13
$L_{\delta r}/I_x$	−5·38±1·08	−5·89±0·97	−5·25±1·07	—	—
N_β/I_z	12·06±2·41	9·86±0·28	10·31±0·40	9·38±0·60	9·21±0·40
N_p/I_z	−0·0066±0·0014	−0·0067±0·0014	−0·0066±0·0014	−0·0066±0·0014	−0·0066±0·0014
N_r/I_z	−0·59±0·12	−0·47±0·089	−0·52±0·094	−0·43±0·099	−0·40±0·094
$N_{\delta r}/I_z$	4·007±0·80	4·05±0·41	4·25±0·47	—	—
a_1	1·076±0·22	0·85±0·048	0·88±0·11	0·82±0·13	0·79±0·13
a_2	0·0012±0·0002	—	—	—	0·0012±0·0002
a_3	−0·0059±0·0012	—	—	—	−0·0059±0·0012
$s^2(\beta)$	—	1·15	0·83	0·11	0·099
$s^2(p)$	—	0·85	—	—	0·24
$s^2(r)$	—	1·49	1·37	0·076	0·074
$s^2(gn_y/V_e)$	—	1·96	1·37	0·33	0·40

results are shown in Figure 5 and column RK1-2 of Table 4. Although the fits to the sideslip, yaw rate, and lateral acceleration records have improved somewhat as shown by the reduced mean square errors (Table 4), they are still not good. At the same time the removal of the p record has removed much of the rolling moment information so that the rolling moment (L) derivatives differ substantially from the results of case RK1-1 and have much larger Cramer-Rao bounds. In addition, the calculated p (unmatched) does not agree very well with the measured record (Fig. 5). The less than good agreement even in the matched records suggests an inadequacy in the mathematical model. Close examination of, say, the sideslip record in Figures 4 or 5 indicates a possible non-linearity with β similar to that noted in Reference 4 when analysing the longitudinal response. The sideslip angle, β, in the present case covers a relatively wide range, i.e. approximately $-5° < \beta < 4°$. The wind tunnel data of Reference 8 does indicate significant changes in, for example, N_β and L_β, over this range of β which would lead to changes in the aircraft response frequency. In Reference 4 it was possible to model the non-linearity of the Pitching Moment curve and thus improve the match. In the present case, a larger number of parameters appears to be involved, and an alternative course is adopted. This is to neglect that initial part of the record where the sideslip angle is large and to analyse a later portion where the sideslip, β, range is smaller and non-linearities less apparent. In Figures 6 and 7 the first 1·85 seconds of record has been removed so that the β range now varies over approximately $-2·3° < \beta < 3·7°$ with the upper value only being attained briefly. In doing this the rudder input no longer appears so that no rudder derivatives can be extracted. In addition, the extrapolated part of the roll rate, p record (Fig. 3*a*) has also been removed. In Figure 6 the sideslip, yaw rate and lateral acceleration have been matched but the roll rate has been excluded while in Figure 7 all four records have been included in the analysis.

The results in columns RK1-3 and RK1-4 of Table 4 together with Figures 6 and 7 show a considerable improvement in the fits obtained. Figure 6 shows almost perfect matching of the sideslip, yaw rate and lateral acceleration records but the agreement between calculated and measured roll rate is still not acceptable, nor are the rolling moment derivatives well identified. In order to improve these areas it seems that the roll rate record needs to be included in the matching process. When this is done, the rolling moment derivatives are much better identified as shown in Table 4 (column RK1-4) and the roll rate fit is also considerably improved (Fig. 7) although some room appears to remain for further improvement. At the same time the sideslip and yaw rate fits have also improved marginally but the lateral acceleration fit has deteriorated slightly. The derivative values identified do not differ all that much from those obtained in case RK1-1 even though the fits are much better. This points to the sensitivity of the time histories to quite small changes in some parameter values.

The results from flight RK2 at $M = 0·72$ appear in Figures 8–10 and in Table 5. The rudder input used is the smoothed curve shown in Figure 2*b*.

TABLE 5
Results from Flight RK2

Item	*A priori*	RK2-1	RK2-2	RK2-3
Y_β/mV_e	$-0{\cdot}292\pm0{\cdot}058$	$-0{\cdot}292\pm0{\cdot}054$	$-0{\cdot}308\pm0{\cdot}055$	$-0{\cdot}290\pm0{\cdot}055$
Y_{δ_r}/mV_e	$-0{\cdot}040\pm0{\cdot}008$	$-0{\cdot}043\pm0{\cdot}008$	$-0{\cdot}042\pm0{\cdot}008$	—
y_β/mV_e	$-0{\cdot}226\pm0{\cdot}045$	$-0{\cdot}190\pm0{\cdot}024$	$-0{\cdot}194\pm0{\cdot}026$	$-0{\cdot}175\pm0{\cdot}029$
y_{δ_r}/mV_e	$-0{\cdot}021\pm0{\cdot}0041$	$-0{\cdot}018\pm0{\cdot}004$	$-0{\cdot}019\pm0{\cdot}004$	—
L_β/I_x	$-25{\cdot}82\pm5{\cdot}2$	$-26{\cdot}43\pm2{\cdot}46$	$-22{\cdot}33\pm4{\cdot}93$	$-23{\cdot}57\pm2{\cdot}55$
L_p/I_x	$-1{\cdot}78\pm0{\cdot}36$	$-2{\cdot}27\pm0{\cdot}28$	$-1{\cdot}90\pm0{\cdot}36$	$-2{\cdot}29\pm0{\cdot}32$
L_r/I_x	$0{\cdot}684\pm0{\cdot}14$	$0{\cdot}741\pm0{\cdot}14$	$0{\cdot}690\pm0{\cdot}14$	$0{\cdot}741\pm0{\cdot}14$
L_{δ_r}/I_x	$-7{\cdot}57\pm1{\cdot}51$	$-8{\cdot}00\pm1{\cdot}03$	$-7{\cdot}51\pm1{\cdot}49$	—
N_β/I_z	$17{\cdot}44\pm3{\cdot}49$	$12{\cdot}56\pm0{\cdot}32$	$12{\cdot}60\pm0{\cdot}46$	$12{\cdot}11\pm0{\cdot}53$
N_p/I_z	$0{\cdot}0126\pm0{\cdot}0025$	$0{\cdot}0126\pm0{\cdot}0025$	$0{\cdot}0126\pm0{\cdot}0025$	$0{\cdot}0126\pm0{\cdot}0025$
N_r/I_z	$-0{\cdot}563\pm0{\cdot}11$	$-0{\cdot}610\pm0{\cdot}084$	$-0{\cdot}639\pm0{\cdot}094$	$-0{\cdot}538\pm0{\cdot}089$
N_{δ_r}/I_z	$5{\cdot}79\pm1{\cdot}16$	$5{\cdot}04\pm0{\cdot}50$	$5{\cdot}17\pm0{\cdot}60$	—
a_1	$1{\cdot}079\pm0{\cdot}22$	$0{\cdot}92\pm0{\cdot}12$	$0{\cdot}92\pm0{\cdot}12$	$0{\cdot}86\pm0{\cdot}14$
$s^2(\beta)$	—	$0{\cdot}51$	$0{\cdot}33$	$0{\cdot}079$
$s^2(p)$	—	$1{\cdot}45(0{\cdot}24)$	—	$0{\cdot}62(0{\cdot}10)$
$s^2(r)$	—	$0{\cdot}42$	$0{\cdot}38$	$0{\cdot}21$
$s^2(gn_y/V_e)$	—	$0{\cdot}69$	$0{\cdot}57$	$0{\cdot}25$

The results mirror closely those obtained from flight RK1 and all the remarks made previously apply here also, although with slightly less emphasis. Figure 8 and column RK2-1 of Table 5 present the results of the full match of all measured variables using the model of Section 2.3 and corresponds to Figure 4 of flight RK1. A relatively good fit all round is obtained but with some residual mismatch obvious. The mean square fit error for p in Table 5 is based on the weighting element 3906 in D_1 while the values in brackets correspond to a D_1 of 657 (see comment following Table 3). In Figure 9 the p record has not been matched and this results in some improvement in the mean square match error of the other three variables (see column RK2-2 of Table 5) but a loss of roll information as previously in case RK1-2. Finally, in Figure 10 all the records are once again matched but the first 1·6 seconds of record removed, including the rudder input history and the roll rate extrapolation of Figure 3*b*. The time history fits are now all good with the corresponding parameters shown in column RK2-3 of Table 5. The values of the extracted parameters are generally not too different from those of case RK2-1 obtained using the full time histories.

4.2 Aerodynamic Derivative Estimates

On examination of the Cramer-Rao bounds, σ_{CR}, of the identified aerodynamic derivatives in Tables 4 and 5 it is possible to classify the derivatives into three groups. In the first group fall those derivatives for which σ_{CR} shows no change from the assigned *a priori* weight, thus implying little or no information regarding these derivatives in the test data. The derivatives in this group are L_r, N_p, and Y_{δ_r}. On the other hand, the group of derivatives showing a substantial change in σ_{CR} are N_β, N_{δ_r}, L_β, and L_{δ_r}. A good deal of confidence can be placed in the identified values of these derivatives. An intermediate group consists of Y_β, L_p and N_r. For these derivatives, some information does exist in the data, leading to some reduction of σ_{CR} relative to the *a priori* weights, but they cannot be regarded as strongly identified as the previous group. This classification is in accord with the groupings identified in Reference 3. The point should be stressed that the above comments only apply when all four time histories are matched simultaneously. If the roll rate record is neglected then the loss of information severely reduces confidence in the rolling moment derivatives.

Looking in more detail at the results of flight RK1 at $M = 0{\cdot}96$ (Table 4), in particular cases RK1-1 and RK1-4 which match all four records, it can be seen that of the strongly identified

derivatives, N_β/I_z, $N_{\delta r}/I_z$, L_β/I_x and $L_{\delta r}/I_x$ only the rudder derivatives $N_{\delta r}/I_z$ and $L_{\delta r}/I_x$ are in reasonable agreement with the *a priori* values, which are based largely on wind tunnel tests. Both of the sideslip derivatives N_β/I_z and L_β/I_x are around 20% less in magnitude than the *a priori* value. Errors in the moments of inertia I_z or I_x would affect the rudder and the sideslip derivatives in a similar manner and hence do not appear to explain the 20% difference. A similar comment applies to corrections for centre of gravity shift. Hence it appears that the differences in the sideslip derivatives reflect genuine aerodynamic differences between flight and wind tunnel associated perhaps with the rapidly changing transonic flowfield and perhaps coupled also with non-linear characteristics with sideslip. The lower values identified here should by used in any mathematical model.

The second, weaker group of derivatives, Y_β/mV_e, L_p/I_x and N_r/I_z also show differences from the *a priori* values. In all cases the flight values are less in magnitude than the corresponding *a priori* value, the difference varying from 10% to as much as 25%. As a result, the damping of the Dutch Roll mode, which is proportional to the sum of these three derivatives, is also well below the *a priori* expectation.

Of the other parameters listed in Table 4, the extracted values of y_β/mV_e and a_1 can be taken with a certain amount of confidence because of the decreased Cramer-Rao bounds relative to the *a priori* weights. The low (in magnitude) value of y_β/mV_e is to some extent a reflection of the extracted values of Y_β and L_β discussed above, as can be seen from the definition of y_β in Equation (22). The value of a_1 on the other hand, is largely a reflection of the sideslip vane calibration factor, G, as defined in Equation (19). Using this definition, the implied value of G is 0·78 for case RK1-1 and 0·74 for case RK1-4. For agreement with wind tunnel calibrations, G should be unity. This large reduction in G compares with the value of 0·84 noted in Reference 4 for the incidence vane at $M = 0{\cdot}96$. While discussing the vane calibrations, the $M = 0{\cdot}72$ results (case RK2) should also be considered. The values of a_1 from Table 5 lead to values for G of 0·86 and 0·80 for the two cases (RK2-1 and RK2-3 respectively) in which all time responses were matched. The equivalent value for the incidence vane at $M = 0{\cdot}71$ from Reference 4 was $G = 1{\cdot}01$. Thus the present results suggest that differences between tunnel and flight are more pronounced for sideslip measurements than for incidence measurements at both subsonic and transonic speeds. More work would be required to resolve these apparent differences.

Turning now to a more detailed examination of the identified aerodynamic derivatives from flight RK2 (Table 5) at $M = 0{\cdot}72$, it may be noted that at this Mach number transonic non-linearities should not yet be apparent so that a reasonable agreement between experiment and theoretical estimates may be expected. Table 6 makes a comparison of the lateral derivatives (excluding the rudder derivatives) obtained from several sources.

TABLE 6
Comparison of M = 0·72 Results

Derivative	*A priori*	Identified	Datcom (Reference 9)	Reference 10
Y_β/mV_e	−0·292	−0·291	−0·22	−0·28
L_β/I_x	−25·82	−26·43 (−23·57)	−33·41	−24·86
L_p/I_x	−1·78	−2·28	−2·03	−2·70
L_r/I_x	0·684	0·741	0·338	0·811
N_β/I_z	17·44	12·34	12·75	10·83
N_p/I_z	0·0126	0·0126	0·045	—
N_r/I_z	−0·563	−0·610 (−0·538)	−0·235	−1·12

The first column in Table 6 lists the *a priori* values, based mainly on wind tunnel tests, for case RK2 at $M = 0{\cdot}72$, while the second column summarises the identified results as in Table 5. These results are the means of columns RK2-1 and RK2-3 except for those cases where the two

columns differ by more than 10% when both results are quoted. Column 3 of Table 6 lists Datcom estimates obtained from Reference 9 and referred to flight at $M = 0{\cdot}70$ with lift coefficient and c.g. position corresponding to flight RK2. Finally, column 4 gives a further set of results, appropriate to the Mirage III, derived from Reference 10.

There appears to be reasonable agreement between the *a priori* and identified values of all derivatives except for L_p, N_β, and N_{δ_r} (Table 5). As with flight RK1 at $M = 0{\cdot}96$, N_β/I_z is less in magnitude than the *a priori* value but in the present case, unlike RK1, L_β/I_x is in good agreement with the *a priori* value. At the same time the Datcom estimate for L_β is approximately 30% high while the estimate from Reference 10 is in good agreement (Table 6). The present value of N_β/I_z is 29% below the *a priori* value while N_{δ_r}/I_z is 13% below (Table 5). If it is assumed that the 13% difference in N_{δ_r}/I_z can be accounted for by an error in the moment of inertia, I_z, this still leaves N_β/I_z about 16% in error. If, however, I_z is assumed to be 13% in error then the theoretical estimates for N_β/I_z in Table 6 would also be reduced by 13% thus spoiling the relatively good agreement between flight and theoretical estimates for N_β. In any case, there remains a significant difference between flight and *a priori* (wind tunnel) values for N_β/I_z at $M = 0{\cdot}72$. The other derivative of interst, L_p, suggests a roll damping in flight almost 30% greater than the *a priori* estimate, opposite to the trend found at $M = 0{\cdot}96$. The agreement with the theoretical estimates is better although the two theoretical estimates differ by over 30%.

Looking at Y_β/mV_e, the agreement between the various sources can be regarded as reasonable but with N_r/I_z the theoretical estimates differ widely with Reference 10 giving a value about twice the measured value and Datcom a value less than half that. This would lead to quite large differences in Dutch Roll damping. Finally, as may perhaps be expected, there are also considerable differences between theoretical and measured values of the weak cross derivatives, L_r and N_p.

4.3 Fin Loads Analysis

As a further example of the use of the modified Newton-Raphson procedure, the method has been applied to the estimation of fin load parameters from flight records of Shear, S, and Tension, T, measurements in the fin. These records were taken concurrently with the records of sideslip, roll rate, yaw rate and lateral acceleration in flights RK1 and RK2 discussed in the preceding sections. The mathematical model used is given in Section 2.4 and the two-part procedure outlined there was used to estimate the parameters of Equation (29). The first part, involving analysis of the aircraft motion has been treated in the preceding sections and the identified parameters summarised in Tables 4 and 5. Those parameters are now held fixed and the corresponding Shear and Tension records analysed separately. The results are summarised in Table 7 and in Figures 11–14.

TABLE 7
Results of Fin Loads Analysis

Item	RK1-1	RK1-4	RK2-1	RK2-3
S_β	$41{\cdot}8 \pm 9{\cdot}4$	$43{\cdot}6 \pm 11{\cdot}1$	$38{\cdot}3 \pm 48{\cdot}1$	$19{\cdot}8 \pm 32{\cdot}0$
S_p	$-2{\cdot}0 \pm 2{\cdot}5$	$-2{\cdot}2 \pm 3{\cdot}0$	$-6{\cdot}2 \pm 14{\cdot}9$	$-12{\cdot}4 \pm 11{\cdot}4$
S_r	$-7{\cdot}5 \pm 5{\cdot}9$	$-15{\cdot}3 \pm 6{\cdot}5$	$-13{\cdot}6 \pm 24{\cdot}8$	$-20{\cdot}9 \pm 17{\cdot}1$
S_{δ_r}	$16{\cdot}5 \pm 5{\cdot}7$	—	$19{\cdot}6 \pm 5{\cdot}8$	—
T_β	$88{\cdot}9 \pm 16{\cdot}9$	$95{\cdot}9 \pm 19{\cdot}9$	$150{\cdot}9 \pm 92{\cdot}4$	$91{\cdot}7 \pm 61{\cdot}3$
T_p	$0{\cdot}27 \pm 4{\cdot}4$	$1{\cdot}06 \pm 5{\cdot}4$	$13{\cdot}6 \pm 28{\cdot}7$	$-4{\cdot}0 \pm 21{\cdot}9$
T_r	$-5{\cdot}2 \pm 10{\cdot}6$	$-17{\cdot}6 \pm 11{\cdot}6$	$16{\cdot}1 \pm 47{\cdot}6$	$-10{\cdot}5 \pm 32{\cdot}7$
T_{δ_r}	$15{\cdot}8 \pm 10{\cdot}2$	—	$21{\cdot}9 \pm 11{\cdot}2$	—
$s^2(S)$	1·34	0·17	0·85	0·47
$s^2(T)$	0·92	0·066	0·54	0·15

Columns RK1-1 and RK1-4 in Table 7 correspond to the same columns in Table 4 and are for flight at $M = 0{\cdot}96$. The equivalent figures are Figures 11 and 12 which should be taken in conjunction with Figures 4 and 7. The fits in Figure 11 display the same features, in particular the apparent phase shifts, as in Figure 4 while Figure 12, where the first 1·85 seconds of record has been removed, shows an excellent fit as did Figure 7. Table 7 shows that, during this manoeuvre, the parameters most strongly identified, judging by the relative magnitudes of the Cramer-Rao bound, σ_{CR}, are the sideslip derivatives and the rudder derivatives (RK1-1 only). There is reasonable agreement for the sideslip derivatives between flight RK1-1 and RK1-4 but the values of the p and r derivatives do vary considerably. It should be remembered that no *a priori* estimates have been assigned to any of the fin load parameters.

From the results of RK1-1 and RK1-4 in Table 7 it is possible to estimate which derivatives, if any, make the greatest contribution to fin loads. This can be done by multiplying each derivative by the maximum value of the corresponding independent variable. For example, the maximum shear due to roll rate would be $S_p \, . \, p_{max}$, etc. When this is done it becomes apparent that, at $M = 0{\cdot}96$ at least, the dominant contribution to both Shear and Tension comes from sideslip with rudder second in importance. For Shear there is also a substantial contribution from yaw rate, r, but this is less apparent with Tension. In both cases the roll rate effect is small.

For $M = 0{\cdot}72$ the results are presented in Table 7 under columns RK2-1 and RK2-3 which correspond to columns RK2-1 and RK2-3 of Table 5. The equivalent figures are Figures 13 and 14 to be taken in conjunction with Figures 8 and 10. As previously, an improved fit is obtained when the initial part of the records, the first 1·6 seconds in this case, is neglected (compare Figure 14 with Figure 13). From Table 7 it appears that most of the derivatives are weakly identified, with the exception of the rudder derivatives and possibly the Tension derivative T_β. If, as before, the contributions to actual fin loads are calculated, the results indicate that Tension forces are once again dominated by sideslip, β, with roll rate, yaw rate and rudder making considerably smaller contributions. With Shear, on the other hand, no dominant contributor appears and it seems that all shear derivatives must be treated equally in this case.

The results obtained here must be regarded as tentative and further work needs to be done (for example to establish some sort of *a priori* structure) to increase confidence in them. Nevertheless, the analysis provides an example of the sort of problem which can be treated by the Modified Newton-Raphson parameter estimation technique.

5. CONCLUDING REMARKS

A modified Newton-Raphson parameter estimation procedure has been applied to the analysis of lateral flight data from a 60° delta wing aircraft at two Mach numbers, $M = 0{\cdot}72$ and $M = 0{\cdot}96$. The response of the aircraft over a period of 5 seconds ($\omega_n T = 17{\cdot}5$) to a rudder pulse was successfully analysed to obtain all the relevant lateral parameters. A data sampling rate of 60 per second ($\omega_n \Delta t = 0{\cdot}06$) was found to be ample and no problems of numerical convergence were encountered. Records of rudder input, sideslip, roll rate, yaw rate and lateral acceleration were used in the analysis of aircraft motion. Neglect of roll rate record was found to degrade the identified results, especially the rolling moment derivatives. It was shown how possible non-linear effects with sideslip can be avoided by basing the identification on those parts of the measured record where sideslip angle was small.

The mathematical model used included, as an integral part, corrections to lateral acceleration measurement for lateral accelerometer position error and also included corrections to sideslip measurements due to vane position error, vane dynamics and possible calibration errors. The results pointed to apparent differences, of considerable magnitude, in sideslip vane calibrations between flight and wind tunnel, which would require further investigation to resolve.

The extracted values of the lateral derivatives obtained in the present study produced a number of differences from the expected values. In particular, the yawing moment due to sideslip, N_β, was found to be significantly lower than expected at both $M = 0{\cdot}72$ and $M = 0{\cdot}96$ while rolling moment due to sideslip, L_β, was low only at $M = 0{\cdot}96$. On the other hand roll damping, L_p, was lower than expected at $M = 0{\cdot}96$ but considerably higher at $M = 0{\cdot}72$. Each of these effects is considered to be largely due to genuine aerodynamic differences as opposed to errors in estimates of moments of inertia or errors in centre of gravity position.

Some comparisons with theoretical estimates was made at $M = 0{\cdot}72$ with generally quite good agreement apart from one or two exceptions.

A further application of the method to the analysis of fin loads, while producing only tentative conclusions, demonstrated the possible adaptation of the identification procedure to a variety of problems. In general the modified Newton-Raphson technique has proved to be an effective and useful tool for aircraft flight test analysis with particular relevance to aircraft mathematical modelling activities.

NOTATION

a_1, a_2, a_3	Coefficients in Equation (19)
A	Matrix of stability parameters, Equation (2)
$\mathbf{b}$	Measurement bias vector
b_o	Equation error bias term, Equation (24)
b_1	Coefficient in Equation (19)
B	Matrix of control parameters, Equation (2)
$\mathbf{c}$	Unknown parameter vector
$\mathbf{c}_o$	Vector of *a priori* parameter values
D_1	Weighting matrix for response variables, Equation (1)
D_2	Weighting matrix for parameter estimates Equation (1)
F	Matrix of stability parameters, Equation (3)
g	Gravitational acceleration
G	Matrix of control parameters, Equation (3) or gain of vane, Equation (15)
h	Height above sea level, m
I_x	Moment of inertia in roll, kg/m^2
I_z	Moment of inertia in yaw, kg/m^2
I_{xz}	Product of inertia, kg/m^2
J	Cost functional (fit error)
K	Constant of proportionality, Equation (16)
L	Rolling moment
L_o	Equation error bias term, Equation (11)
m	Mass, kg
M	Mach number
$\mathbf{n}$	Measurement noise vector
N	Number of data samples or yawing moment
N_o	Equation error bias term, Equation (11)
n_y	Lateral acceleration in g units
p	Roll rate, rad/s
q	Pitch rate, rad/s
r	Yaw rate, rad/s
S	Reference area, m^2, or Shear force in fin
S_o	Bias term, Equation (28)

s^2	Mean square weighted error
t	Time, sec
T	Record length, sec, or Tension force in fin
T_o	Bias term, Equation (28)
$\mathbf{u}$	Vector of control input variables
v	Velocity increment in y-direction, m/s
V	Resultant airspeed, m/s
w	Velocity increment in z-direction, m/s
x	Body axis co-ordinate in forward direction
$\mathbf{x}$	Vector of state variables
y	Body axis co-ordinate in lateral direction
$\mathbf{y}$	Vector of response variables, Equation (3)
Y	Force in y-direction, N
Y_o	Equation error bias term, Equation (11)
$y_\beta, y_p, y_r, y_{\delta_r}$	Modified sideforce derivatives, Equation (22)
y_o	Equation bias term, Equation (24)
z	Body axis co-ordinate in downward direction
$\mathbf{z}$	Measured response vector, Equation (4)
α	Angle of incidence increment, rad
β	Sideslip angle, rad
β_d	Inertial correction to β, Equation (16)
β_s	Roll and yaw rate correction to β, Equation (14)
Δ	Increment
δ_a	Aileron angle, rad
δ_e	Elevator angle increment, rad
δ_r	Rudder angle, rad
θ	Pitch attitude increment, rad
ρ	Air density, kg/m^3
σ	Standard deviation
σ_{CR}	Cramer-Rao Bound
ϕ	Roll attitude, rad
ω_n	Natural undamped frequency, rad/s

Subscripts

a	Lateral accelerometer
e	Trim or equilibrium state
i	Time index
m	Measured value
p	Derivative w.r.t. p

r	Derivative w.r.t. r
v	Sideslip vane
β	Derivative w.r.t. β
$\dot{\beta}$	Derivative w.r.t. $\dot{\beta}$
δ_a	Derivative w.r.t. δ_a
δ_r	Derivative w.r.t. δ_r

REFERENCES

1. Iliff, K. W., and Taylor, L. W. Jr. Determination of Stability Derivatives from Flight Data Using a Newton-Raphson Minimisation Technique. NASA TN D-6579, March 1972.
2. Taylor, L. W. Jr., and Iliff, K. W. Systems Identification Using a Modified Newton-Raphson Method—A Fortran Program. NASA TN D-6734, May 1972.
3. Feik, R. A. Aircraft Mathematical Model Validation—Comments on the Use of a Systems Identification Procedure. ARL/Aero Note 365, August 1976.
4. Feik, R. A. Longitudinal Aerodynamics Extracted from Flight Tests Using a Parameter Estimation Method ARL/Aero Note 379, October 1978.
5. Wolowicz, C. H. Considerations in the Determination of Stability and Control Derivatives and Dynamic Characteristics from Flight Data. AGARD Report 549, Part I, 1966.
6. Forsyth, G. F. Transonic Wind Tunnel Tests of a Dual System (Vanes, Pressure Taps) Gust Probe and a Pitot-Static Probe Mounted Side by Side. ARL/Aero. Note 334, January 1972.
7. Park, G. D. Parameter Identification Technology Used in Determining In-Flight Airload Parameters. *Journal of Aircraft*, Vol. 14, No. 3, March 1977.
8. Pollock, N., and Forsyth, G. Wind Tunnel Measurements of the Longitudinal and Lateral Characteristics of a Mirage 1110 Model at Subsonic, Transonic and Supersonic Speeds. ARL/Aero. Note 319, January 1970.
9. Hoak, D. E., *et al.* USAF Stability and Control Datcom. AFFDL, October 1960. Revised to June 1977.
10. Wanner, J. C. Dynamique du Vol et Pilotage des Avions. ONERA Publication No. 1976-6.

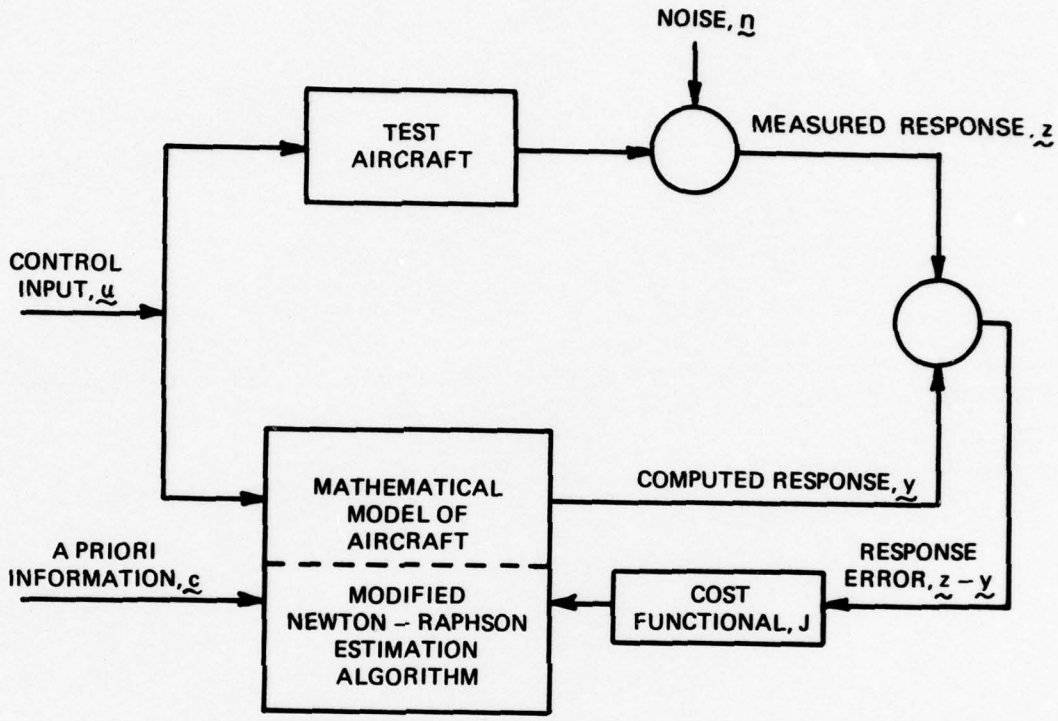

FIG. 1. BASIC CONCEPT OF ESTIMATION METHOD

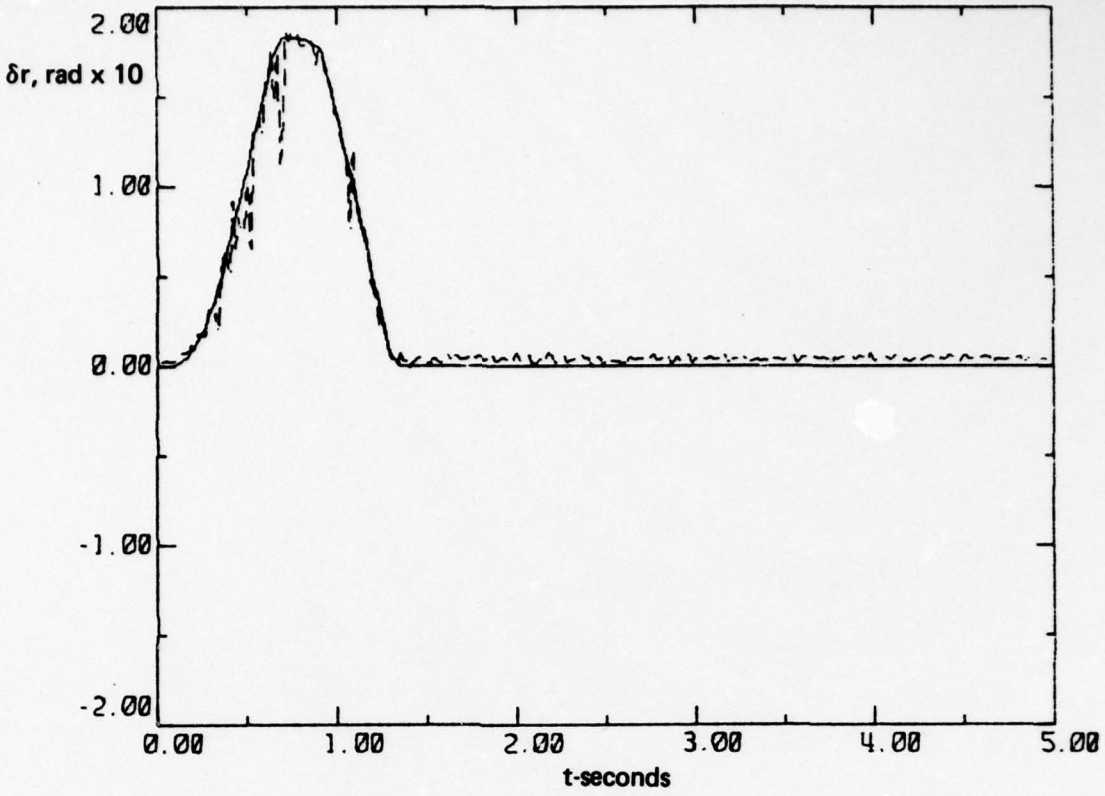

(a) Flight RKI

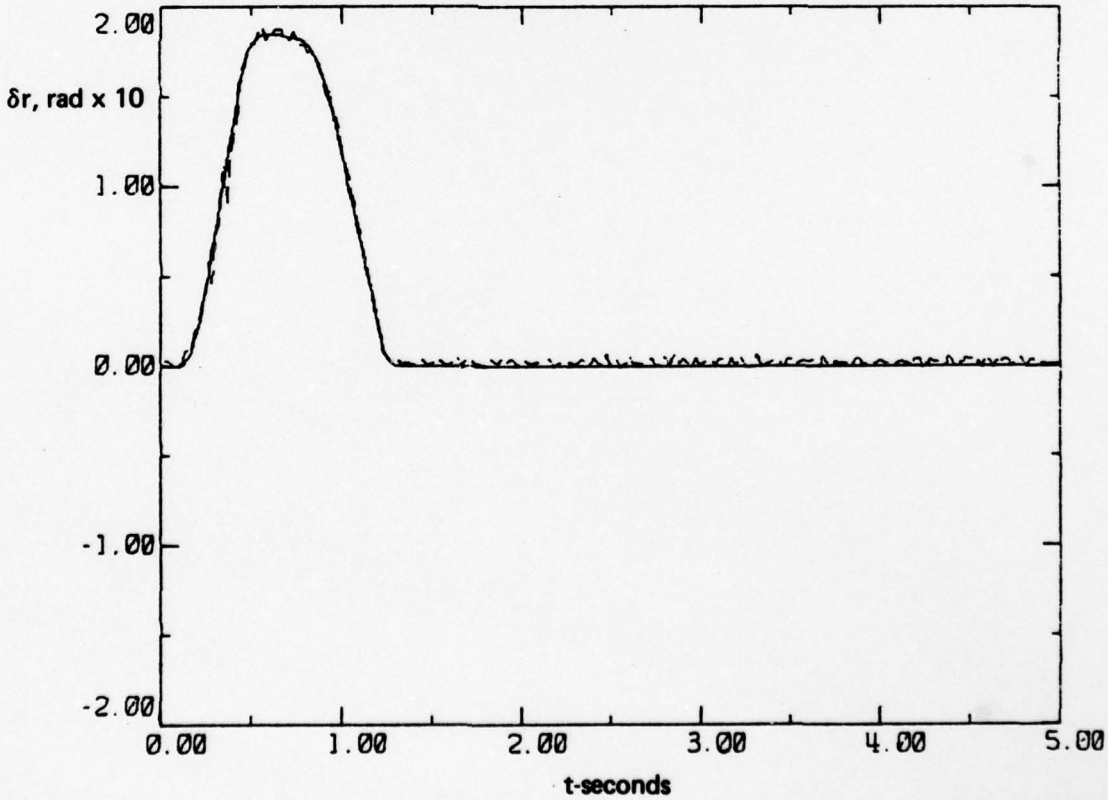

(b) Flight RK2

FIG. 2. SMOOTHED RUDDER INPUT

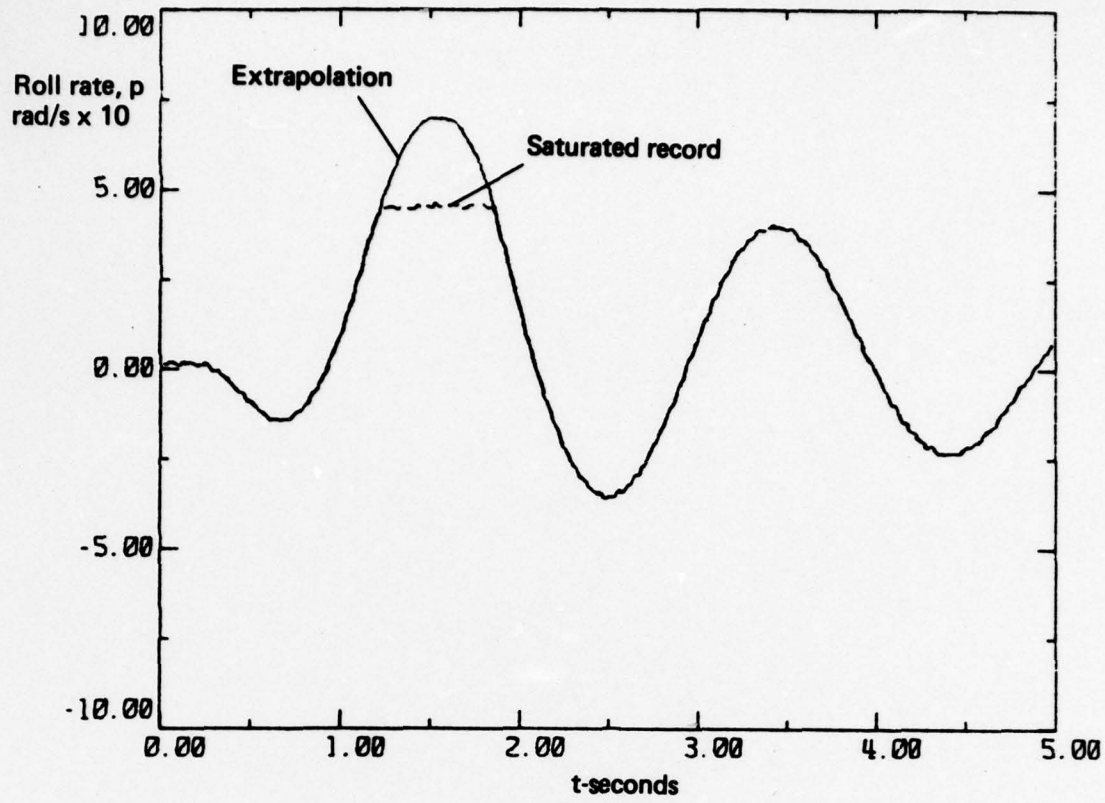

(a) Flight RKI

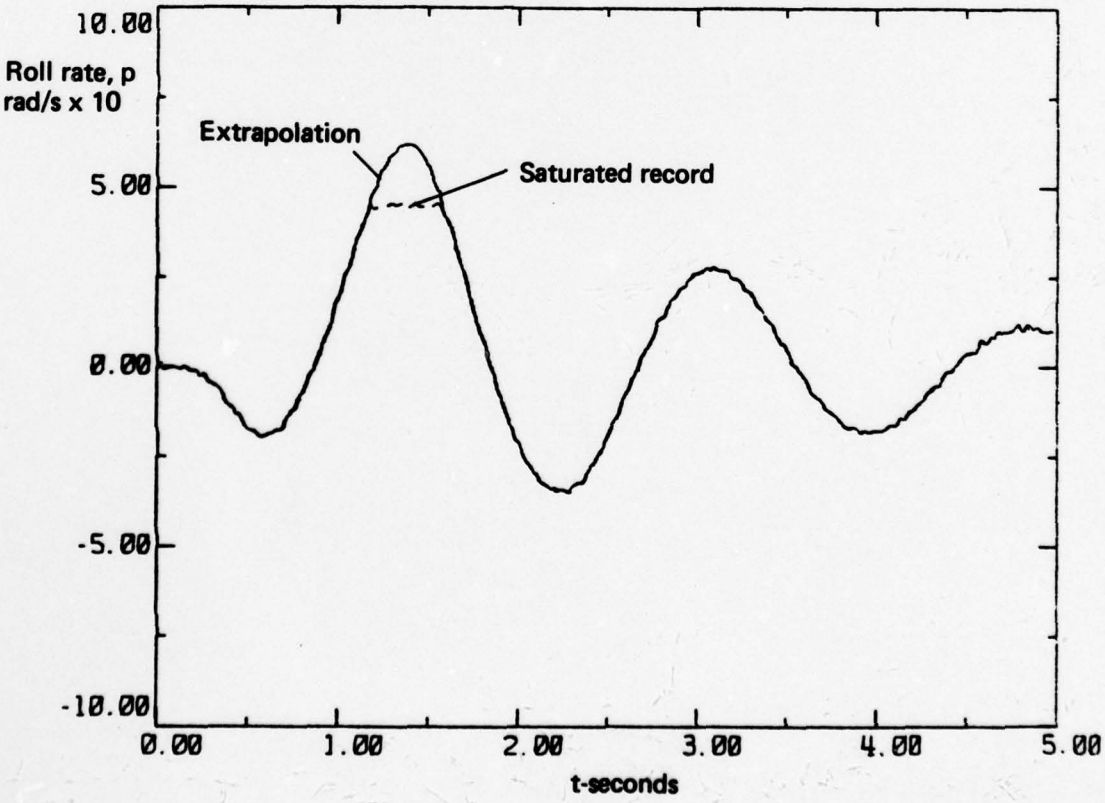

(b) Flight RK2

FIG. 3. EXTRAPOLATION OF ROLL RATE RECORD

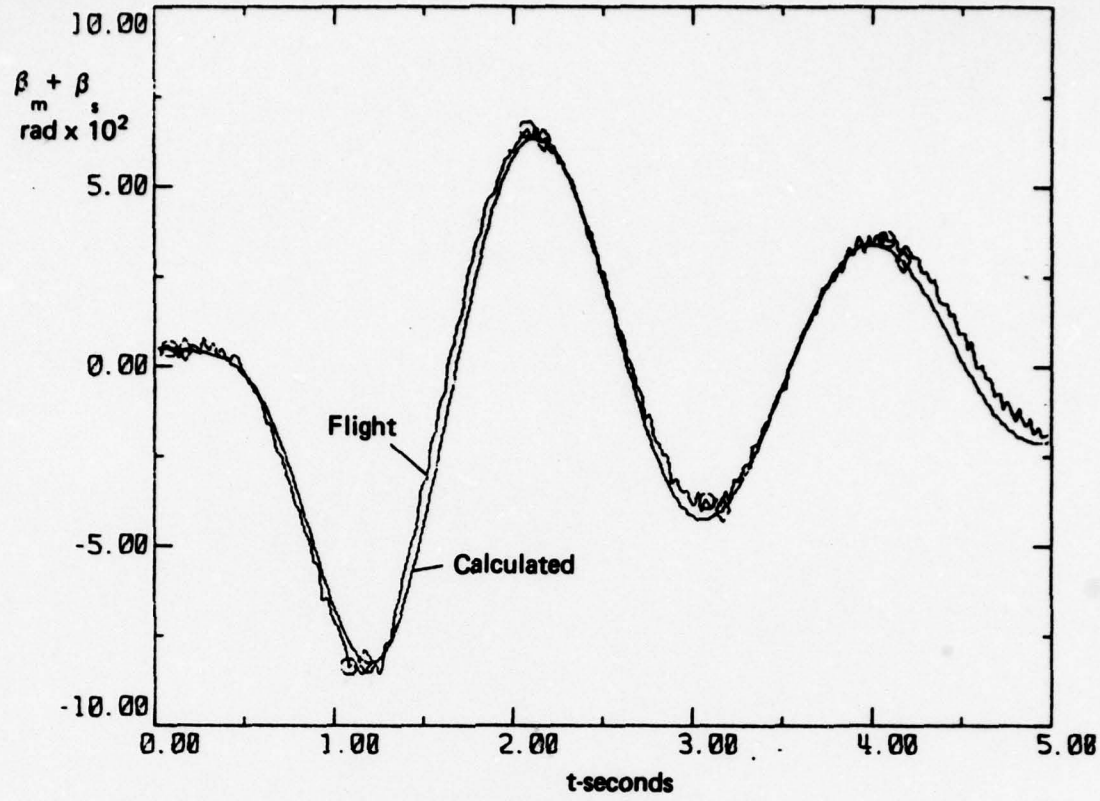

(a) Corrected slideslip angle

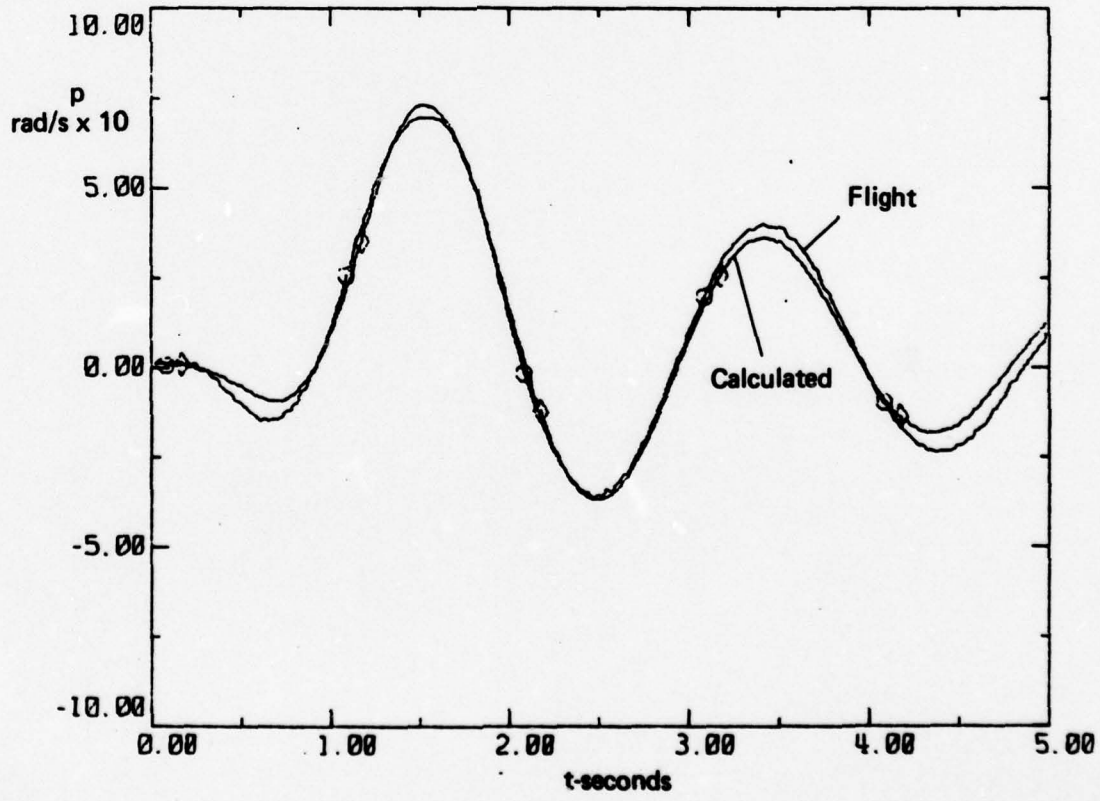

(b) Roll rate

FIG. 4. MATCHED RESULTS – CASE RKI – 1, $\underline{z} = (\beta_m + \beta_s, p, r, gn_y/Ve)$

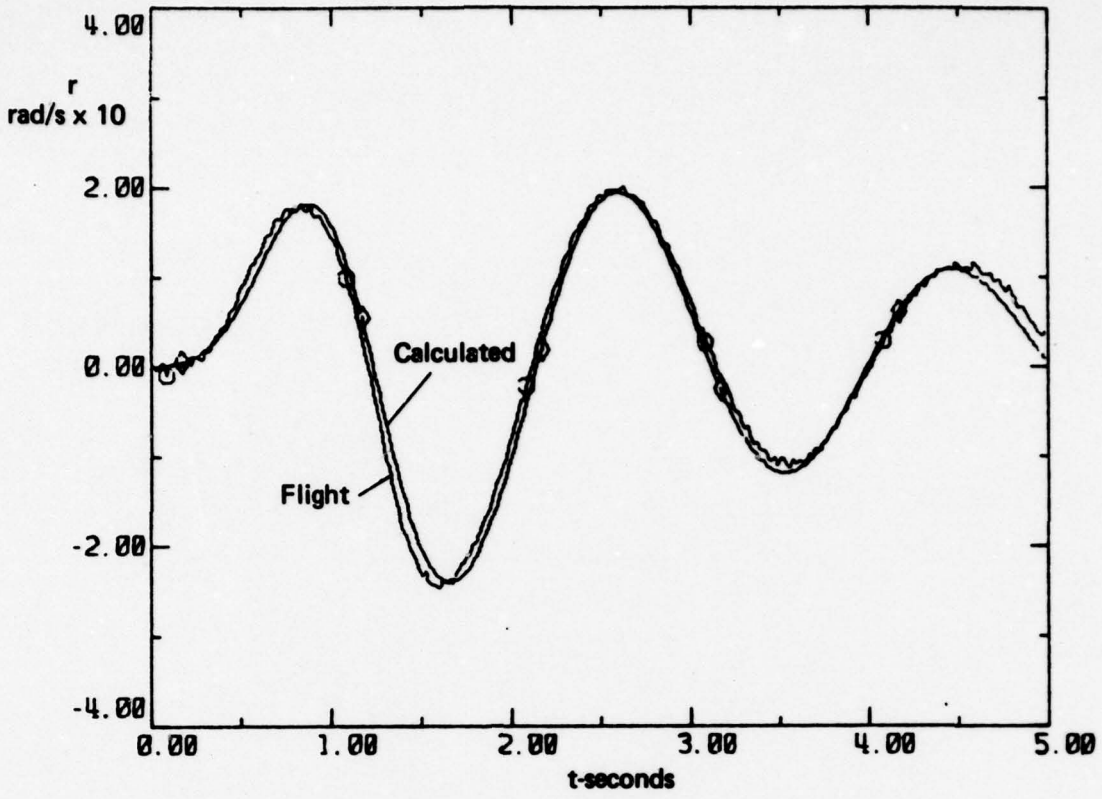

(c) Yaw rate

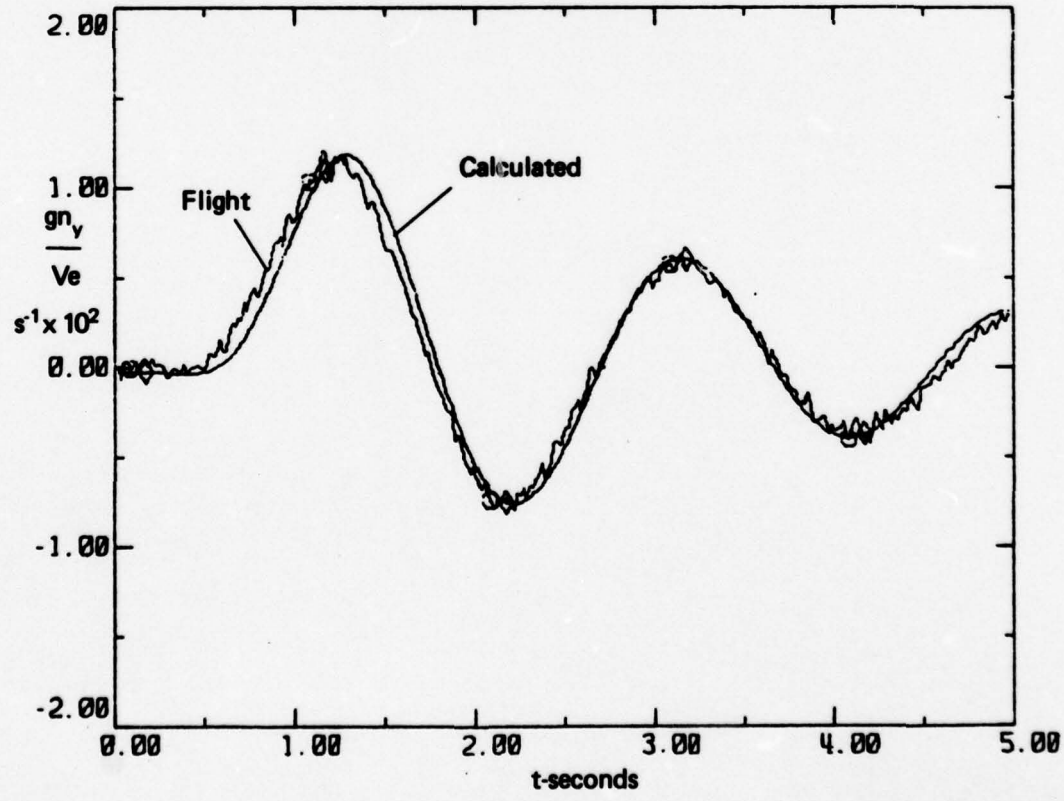

(d) Lateral acceleration

Fig. 4. (cont.)

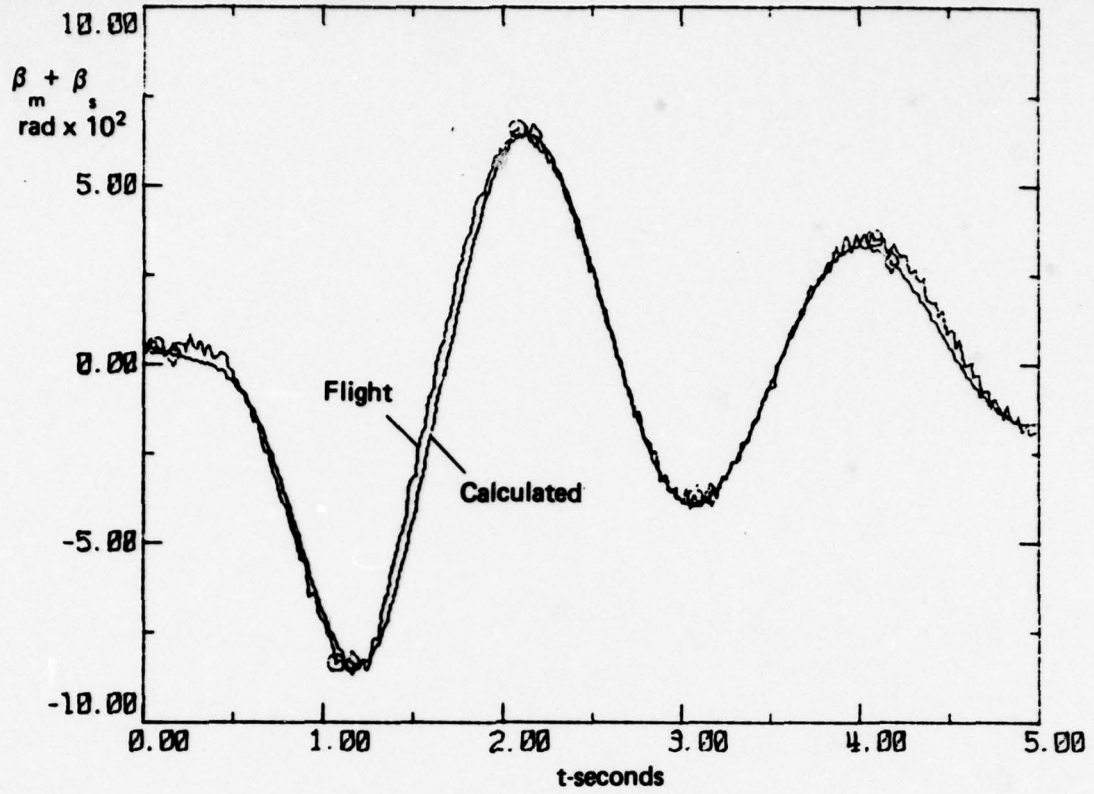

(a) Corrected slideslip angle

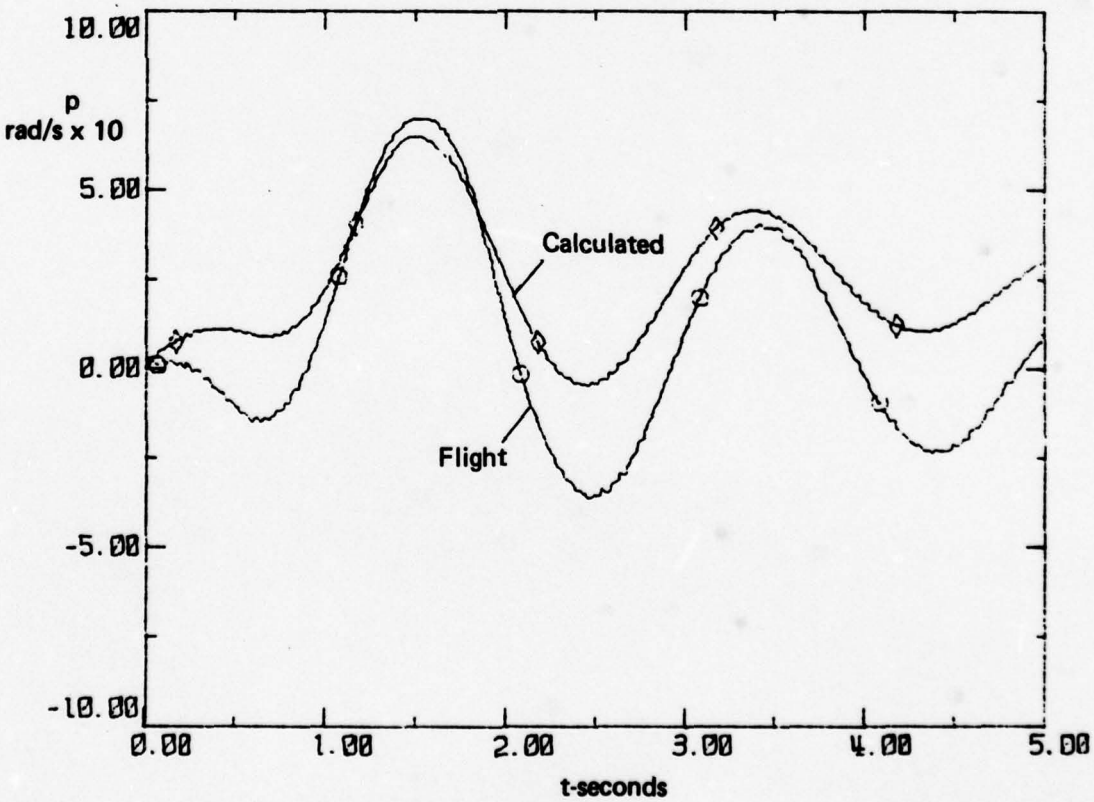

(b) Roll rate

FIG. 5. MATCHED RESULTS – CASE RKI – 2, $\underset{\sim}{z} = (\beta_m + \beta_s, r, gn_y/Ve)$

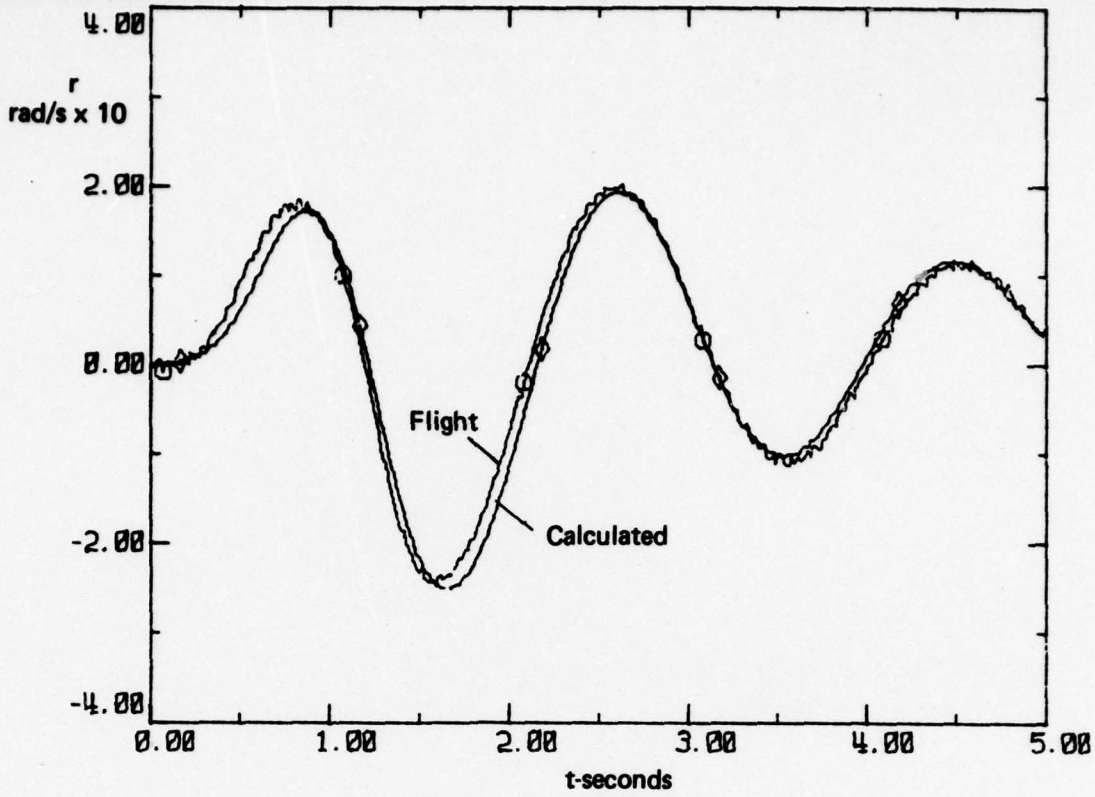

(c) Yaw rate

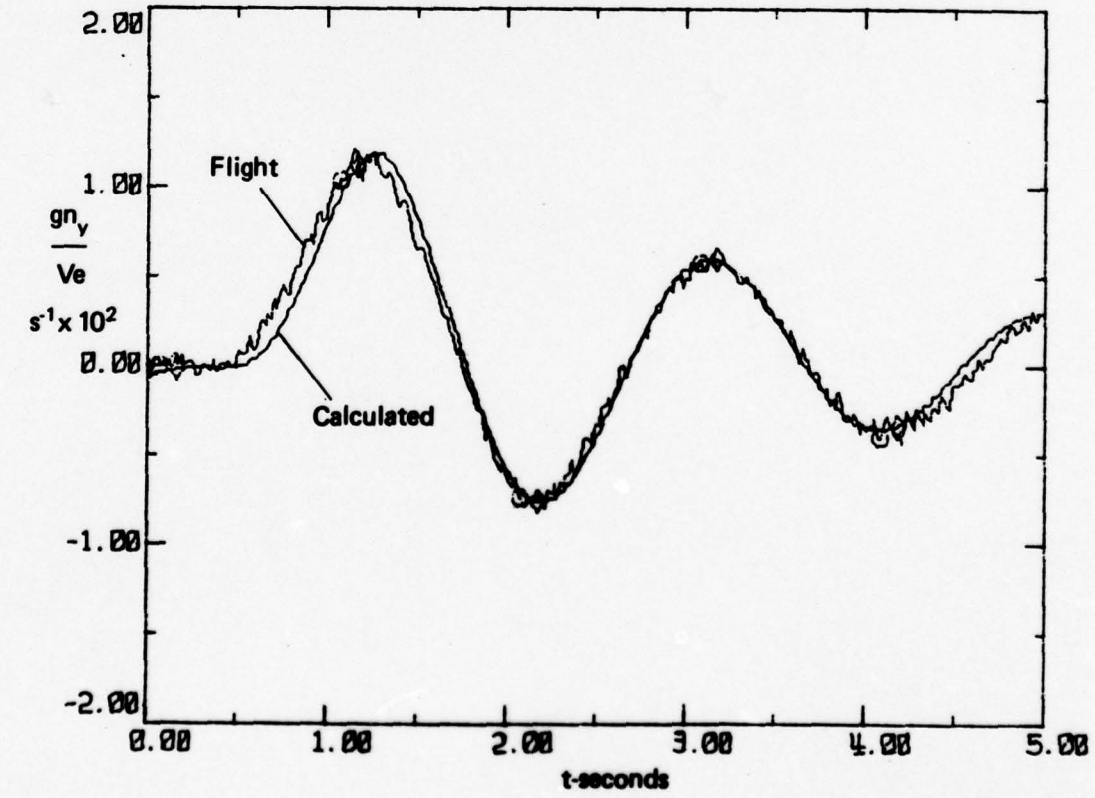

(d) Lateral acceleration

Fig. 5. (cont.)

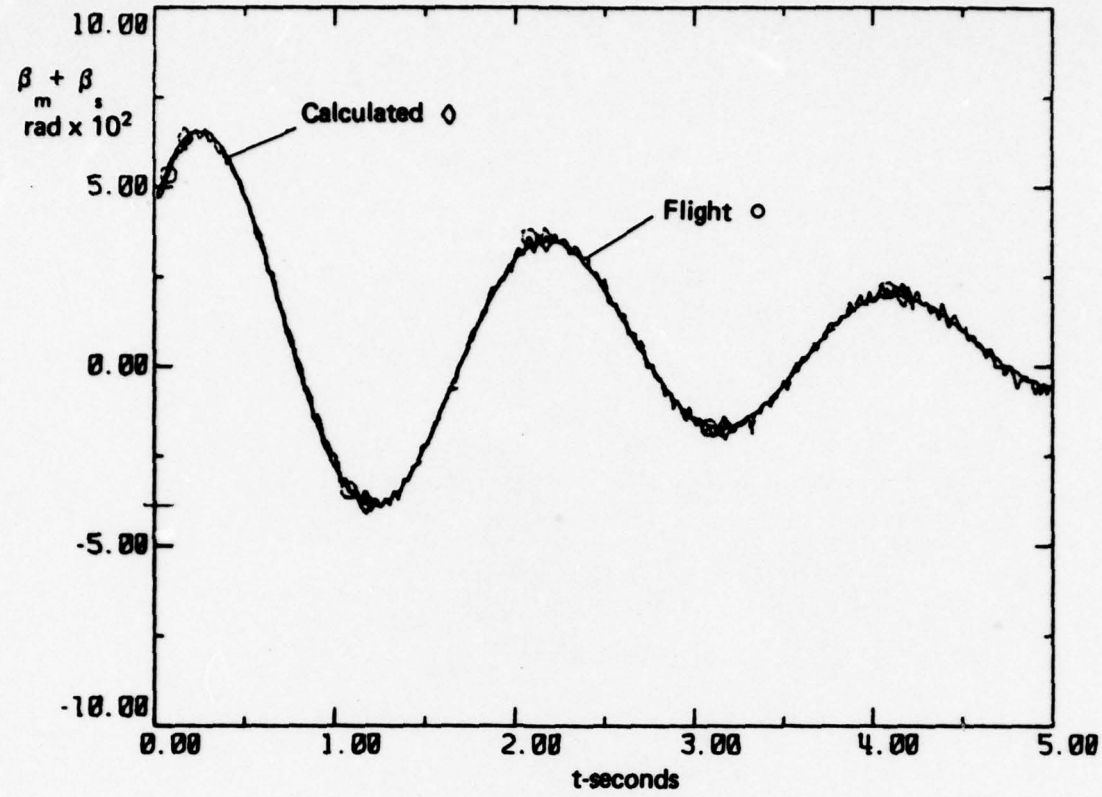

(a) Corrected slideslip angle

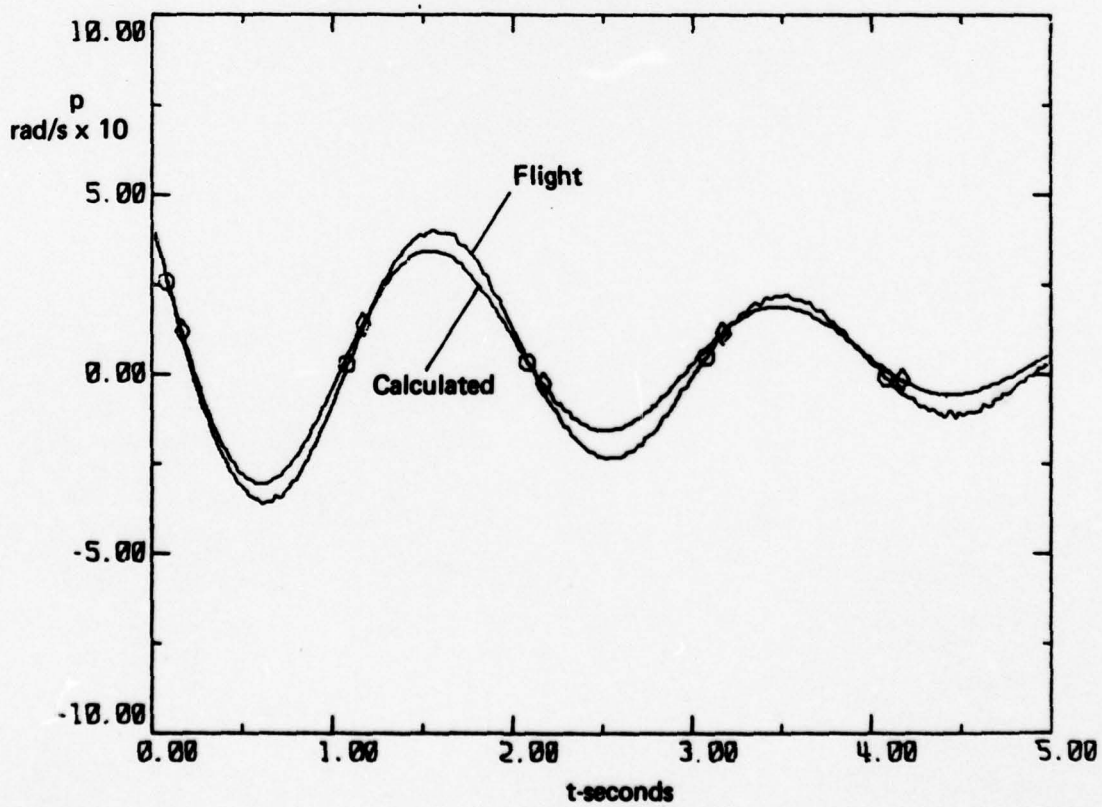

(b) Roll rate

FIG. 6. MATCHED RESULTS – CASE RKI – 3, $\underline{z} = (\beta_m + \beta_s, p, r, gn_y/Ve)$

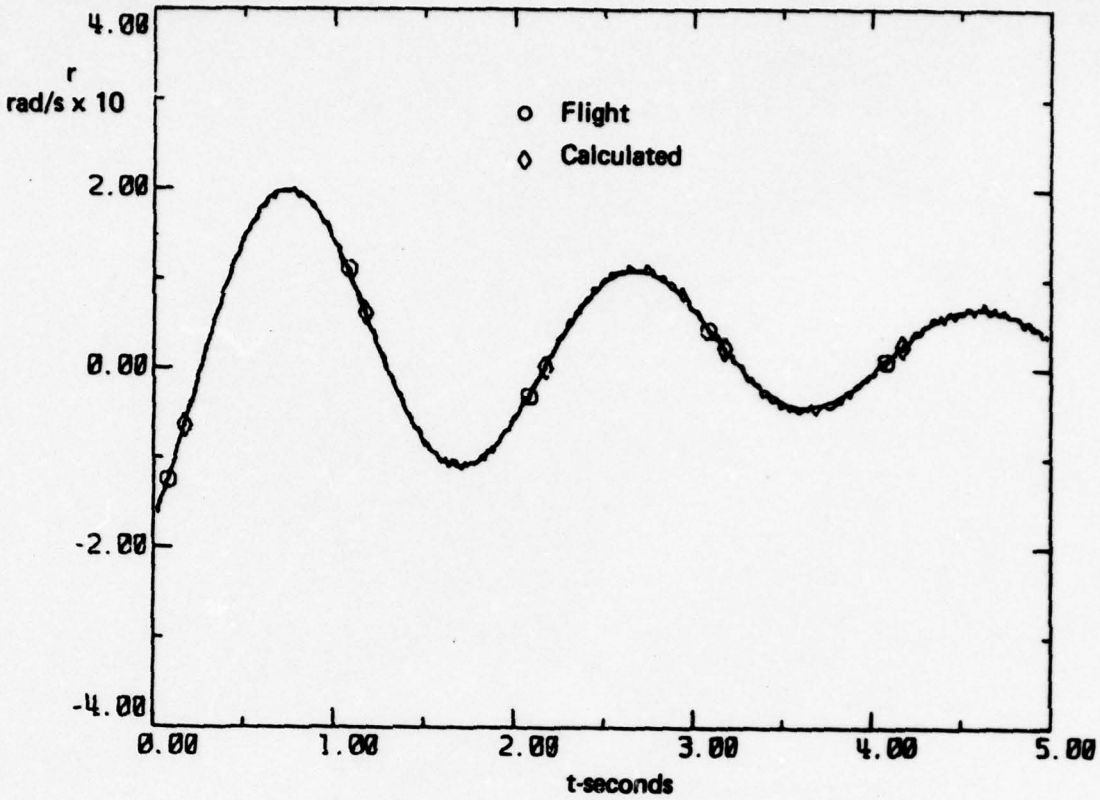

(c) Yaw rate

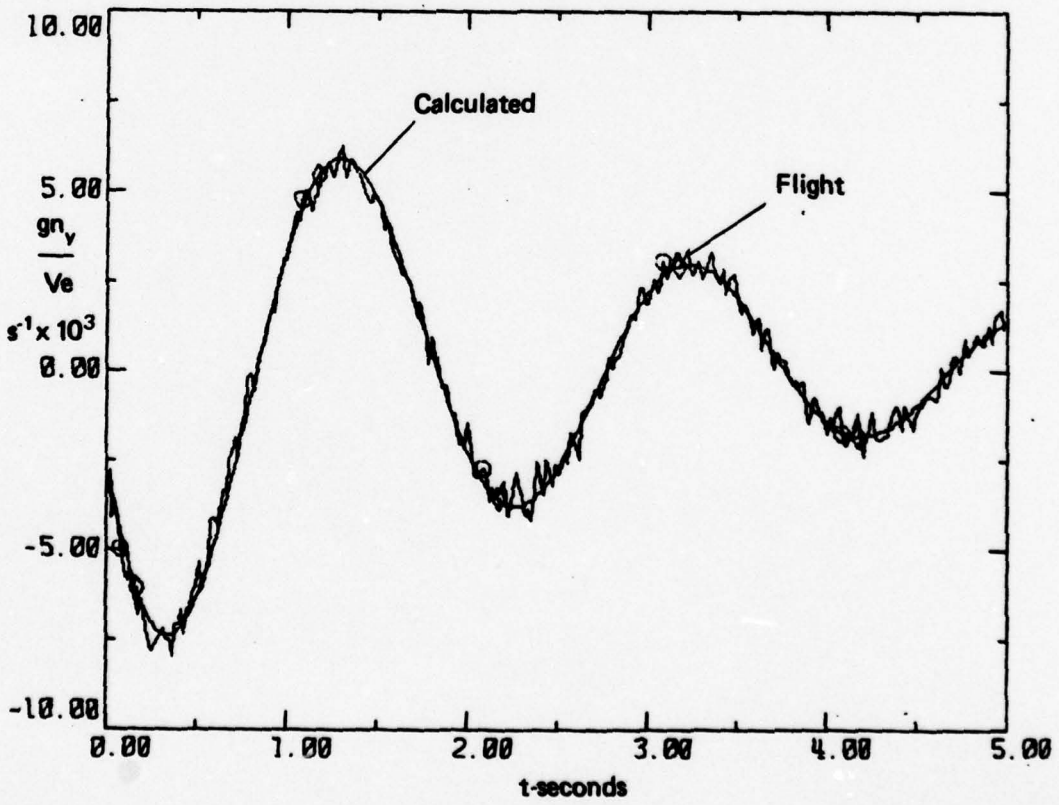

(d) Lateral acceleration

Fig. 6. (cont.)

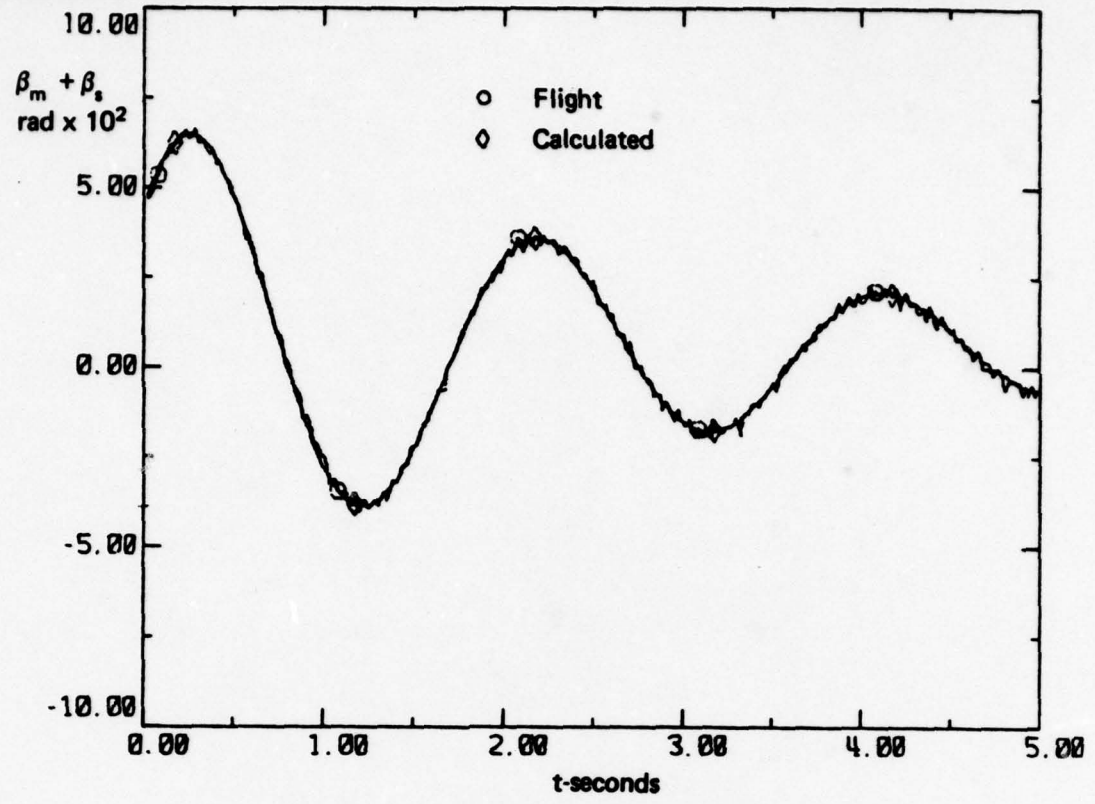

(a) Corrected slideslip angle

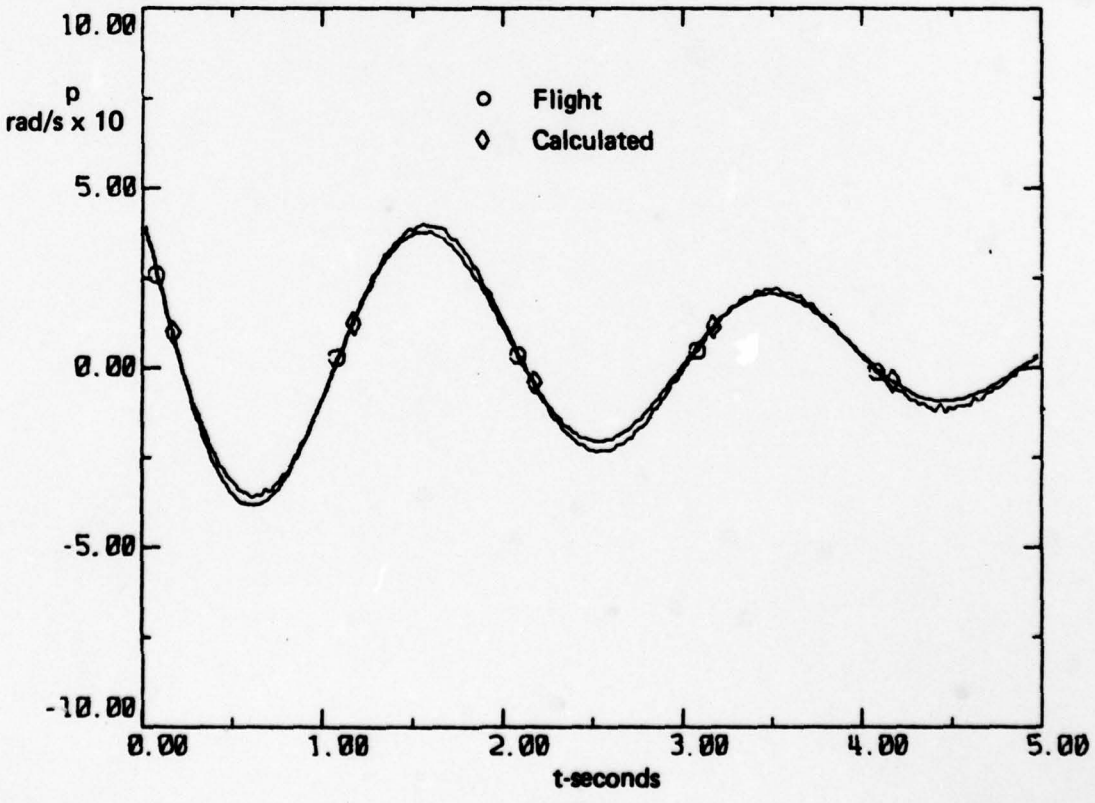

(b) Roll rate

FIG. 7. MATCHED RESULTS – CASE RKI – 4, $\underset{\sim}{z} = (\beta_m + \beta_s, p, r, gn_y/Ve)$

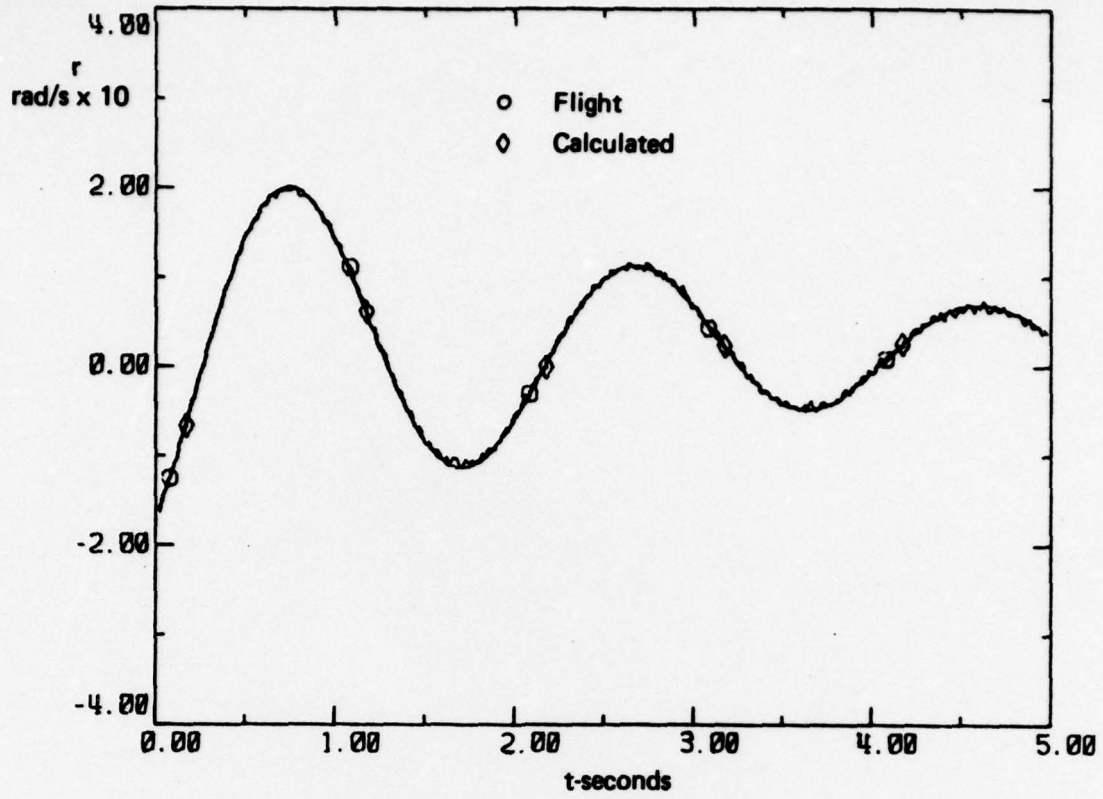

(c) Yaw rate

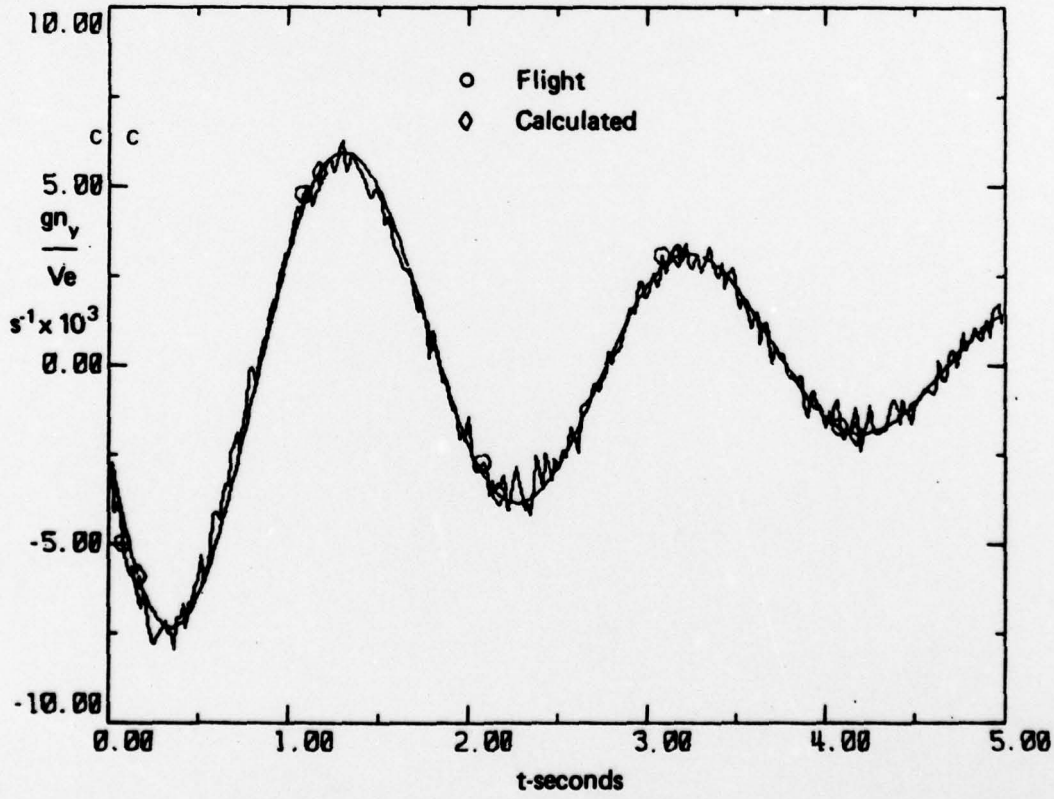

(d) Lateral acceleration

Fig. 7. (cont.)

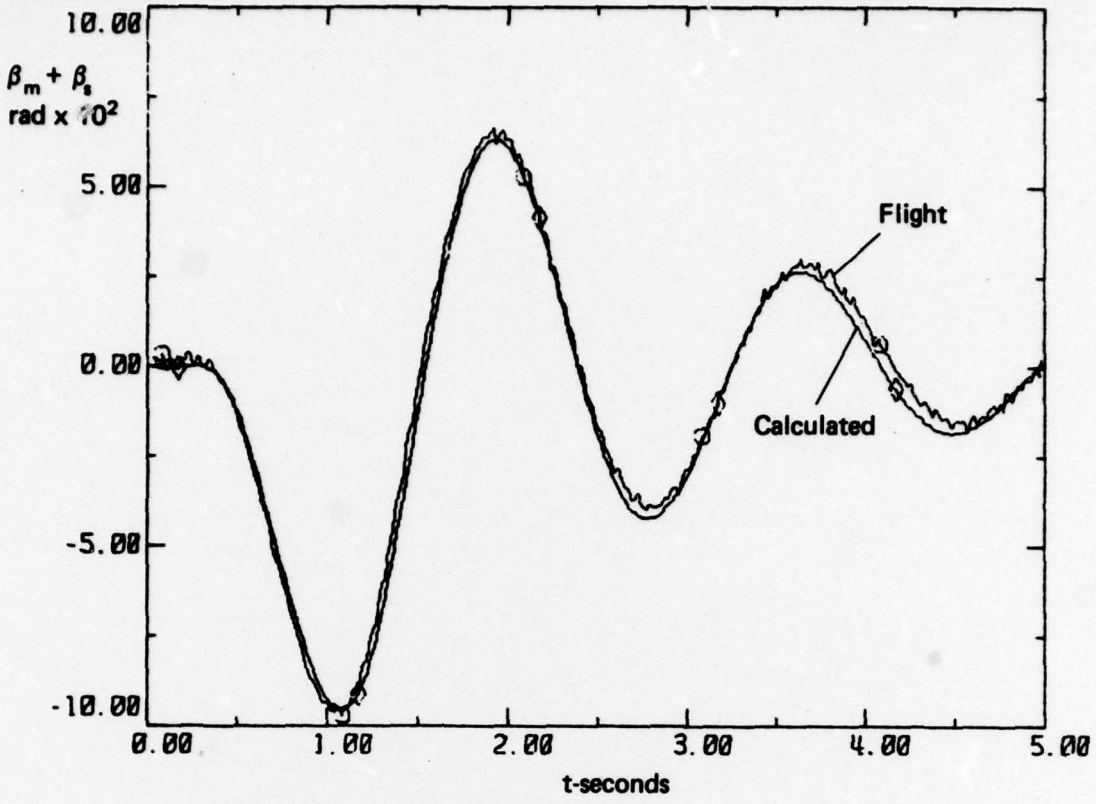

(a) Corrected slideslip angle

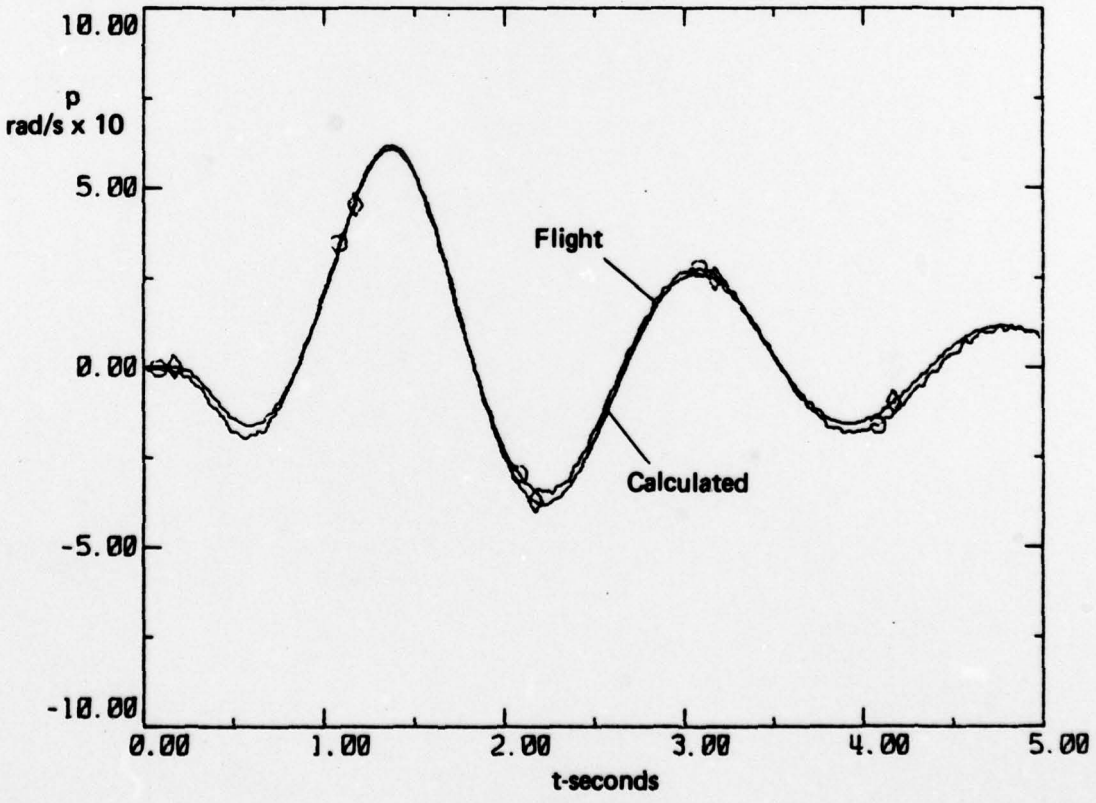

(b) Roll rate

FIG. 8. MATCHED RESULTS – CASE RK2 – 1, $\underset{\sim}{z} = (\beta_m + \beta_s, p, r, gn_y/Ve)$

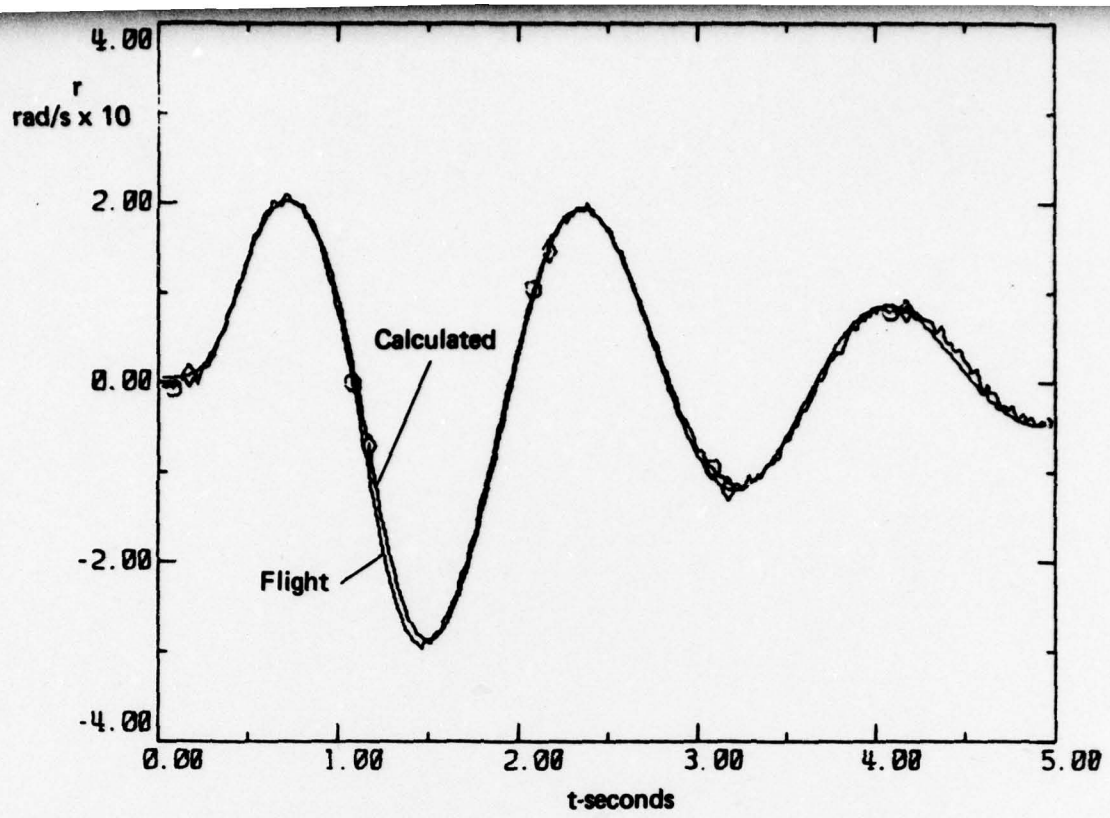

(c) Yaw rate

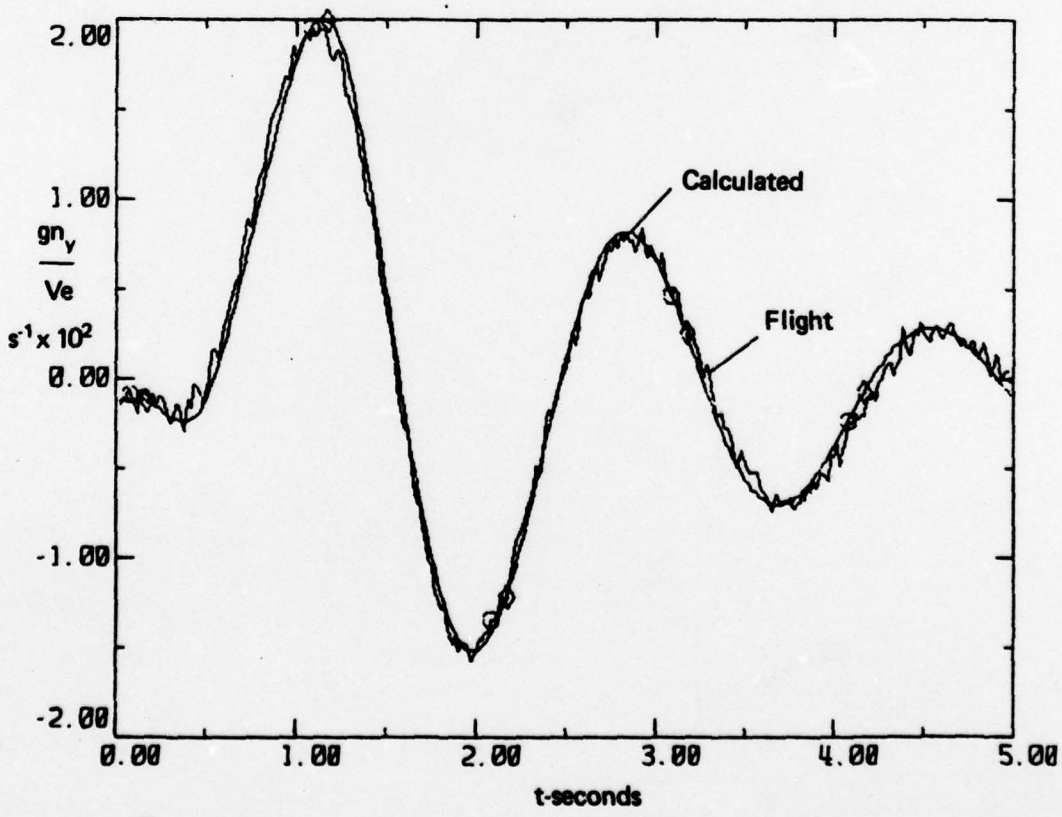

(d) Lateral acceleration

Fig. 8. (cont.)

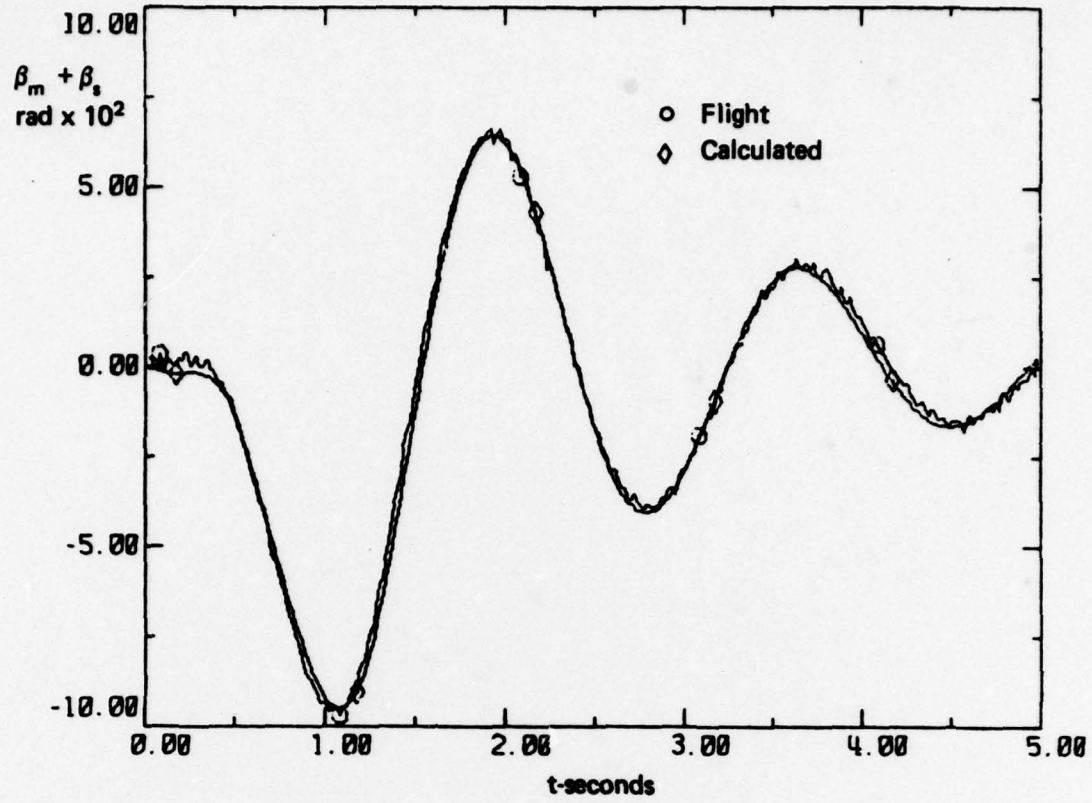

(a) Corrected slideslip angle

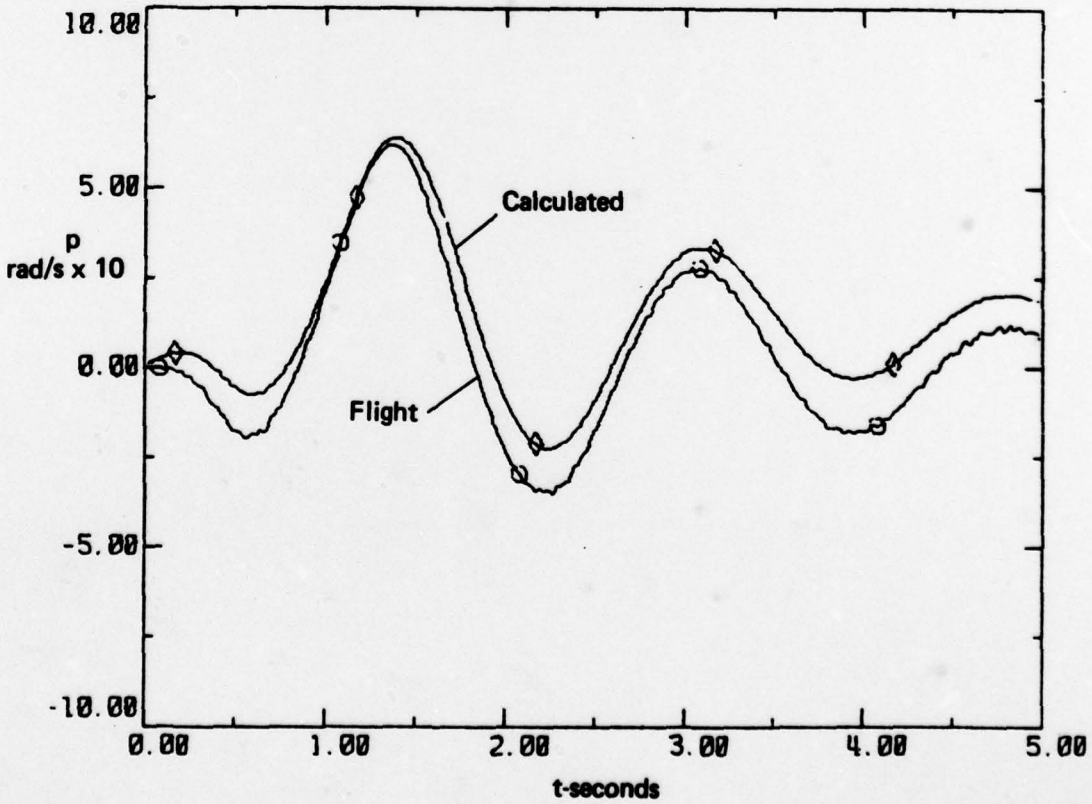

(b) Roll rate

FIG. 9. MATCHED RESULTS – CASE RK2 – 2, $\underline{z} = (\beta_m + \beta_s, r, gn_y/Ve)$

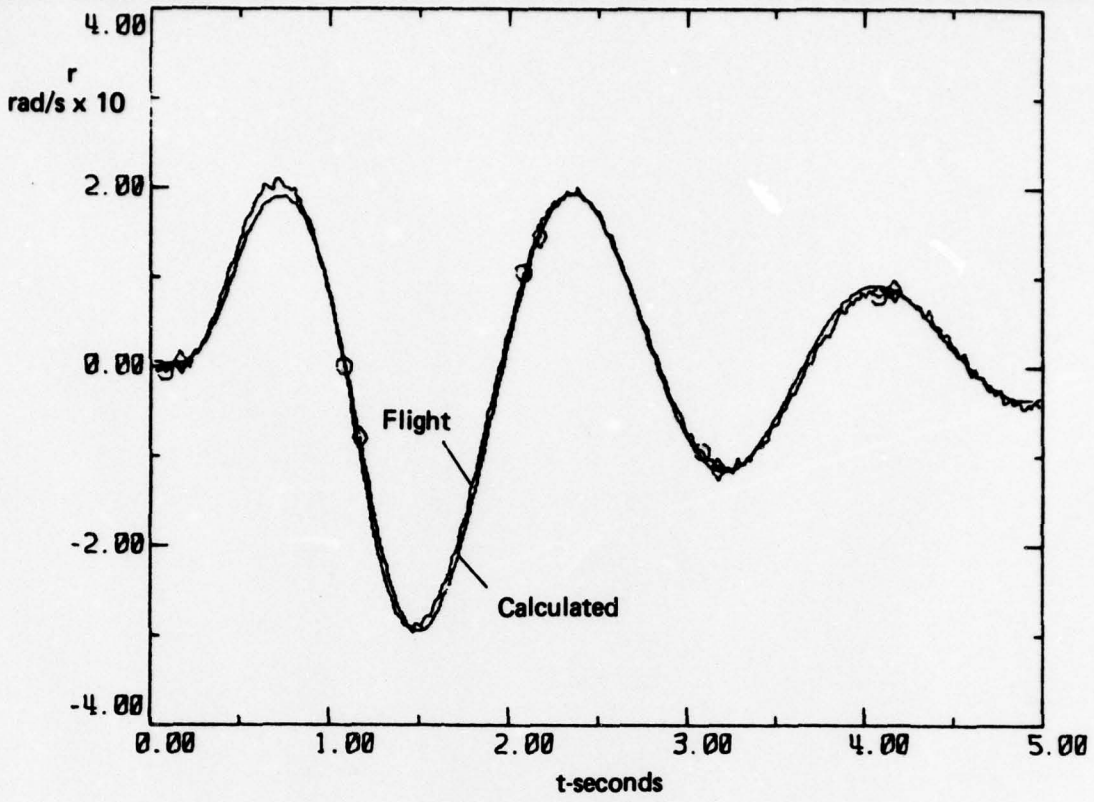

(c) Yaw rate

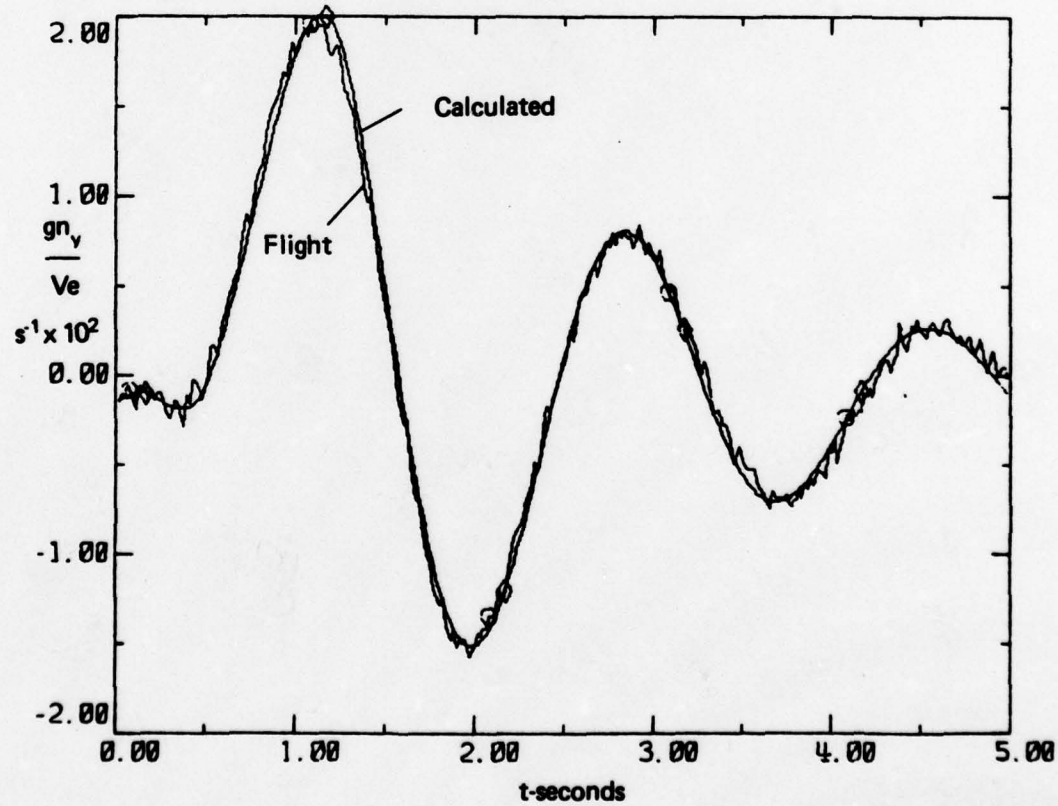

(d) Lateral acceleration

Fig. 9. (cont.)

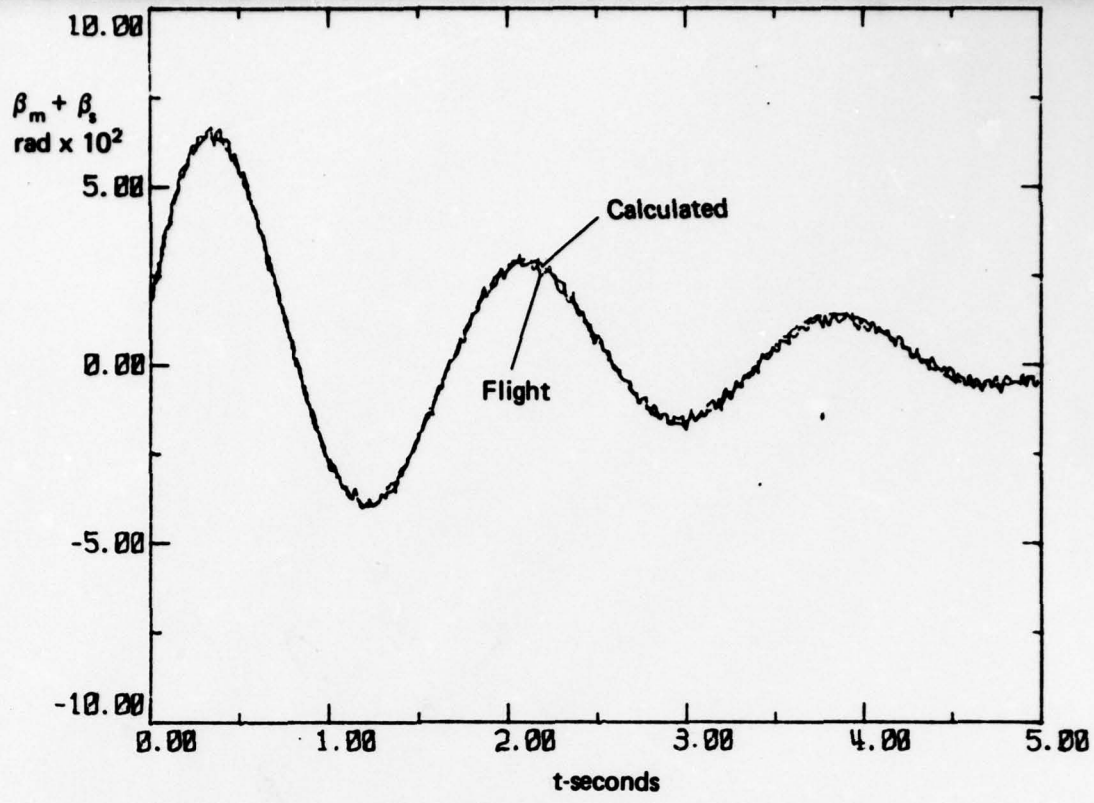

(a) Corrected slideslip angle

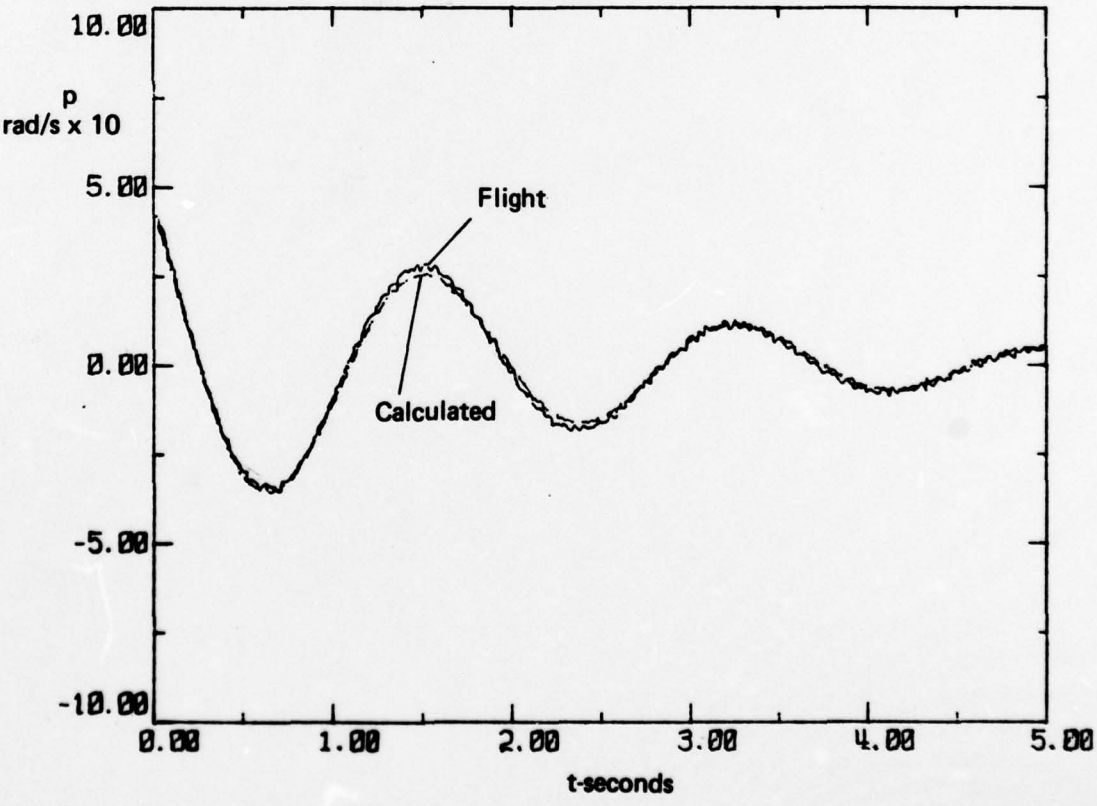

(b) Roll rate

FIG. 10. MATCHED RESULTS – CASE RK2 – 3, $\underline{z} = (\beta_m + \beta_s, p, r, gn_y/Ve)$

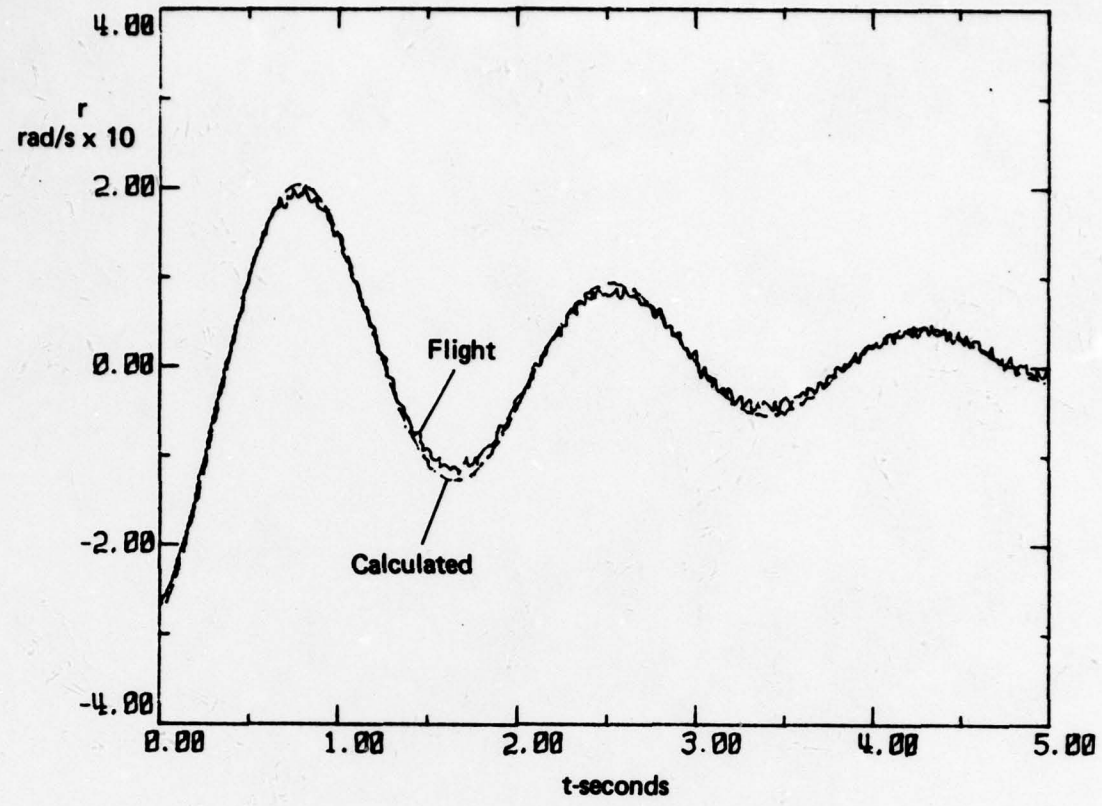

(c) Yaw rate

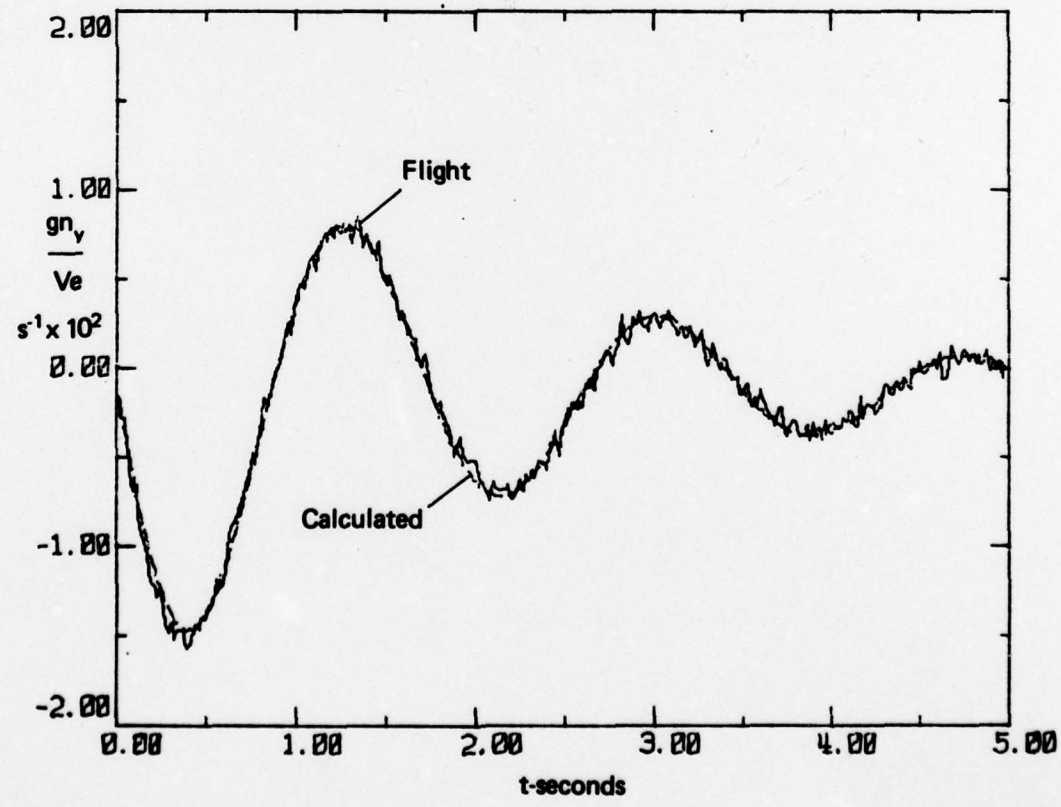

(d) Lateral acceleration

Fig. 10. (cont.)

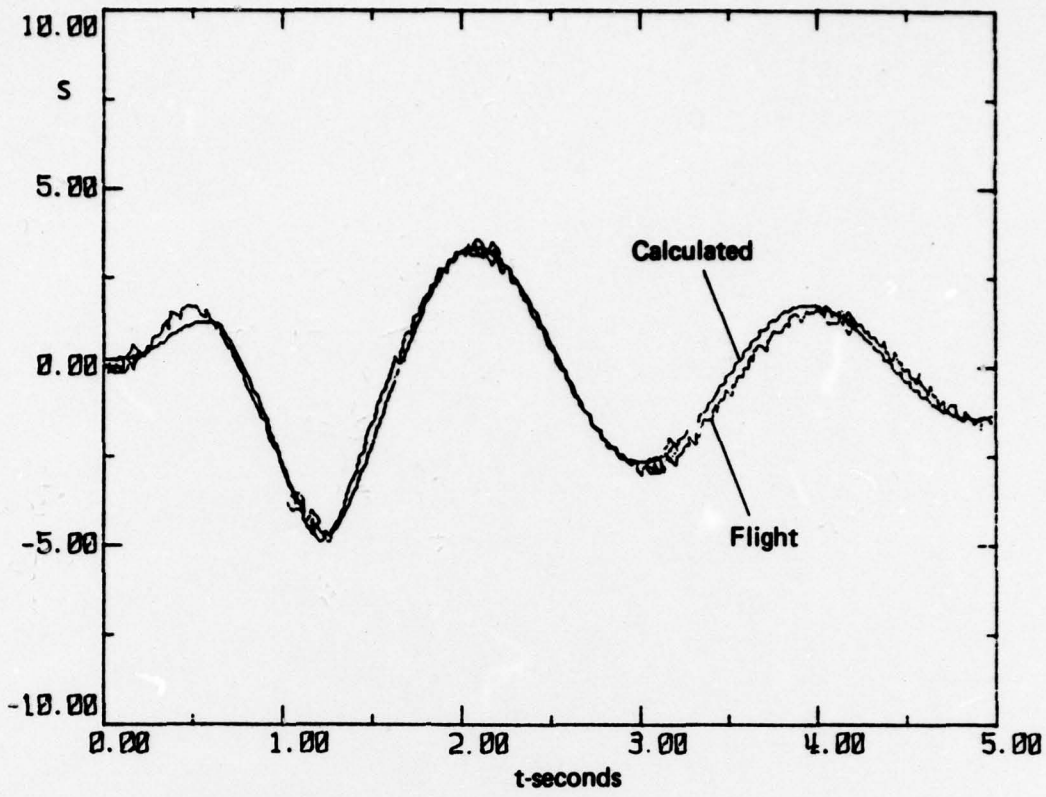

(a) Shear

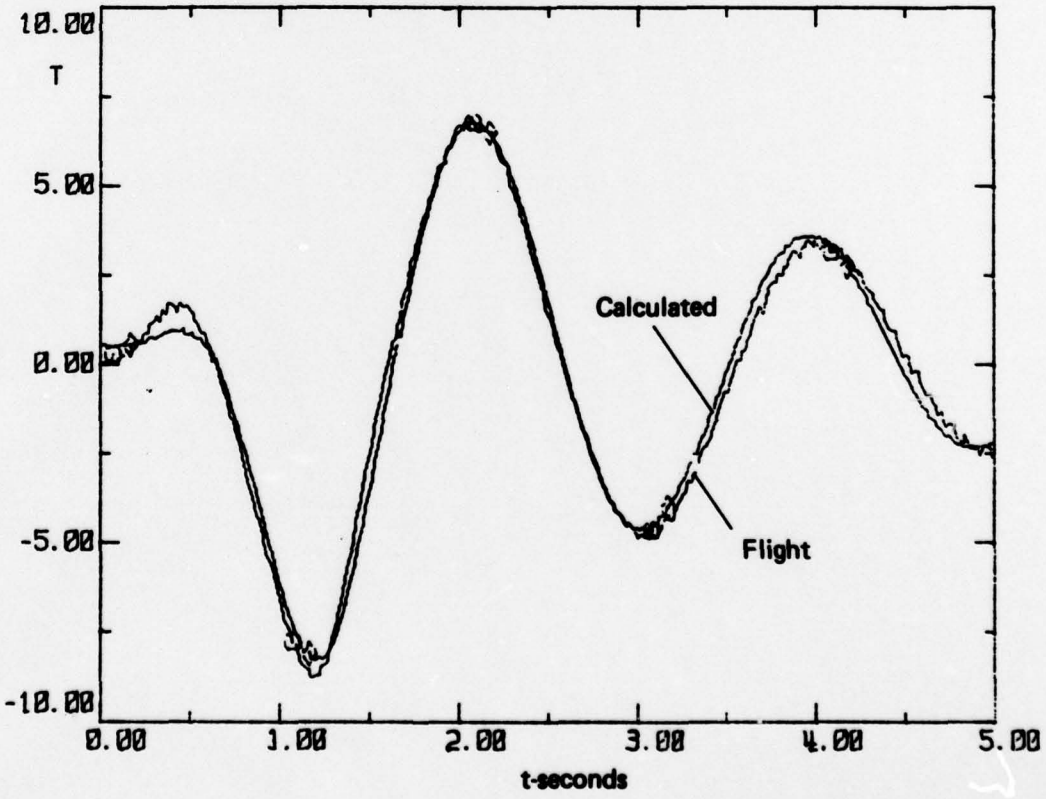

(b) Tension

FIG. 11. MATCHED FIN LOADS – RKI – I

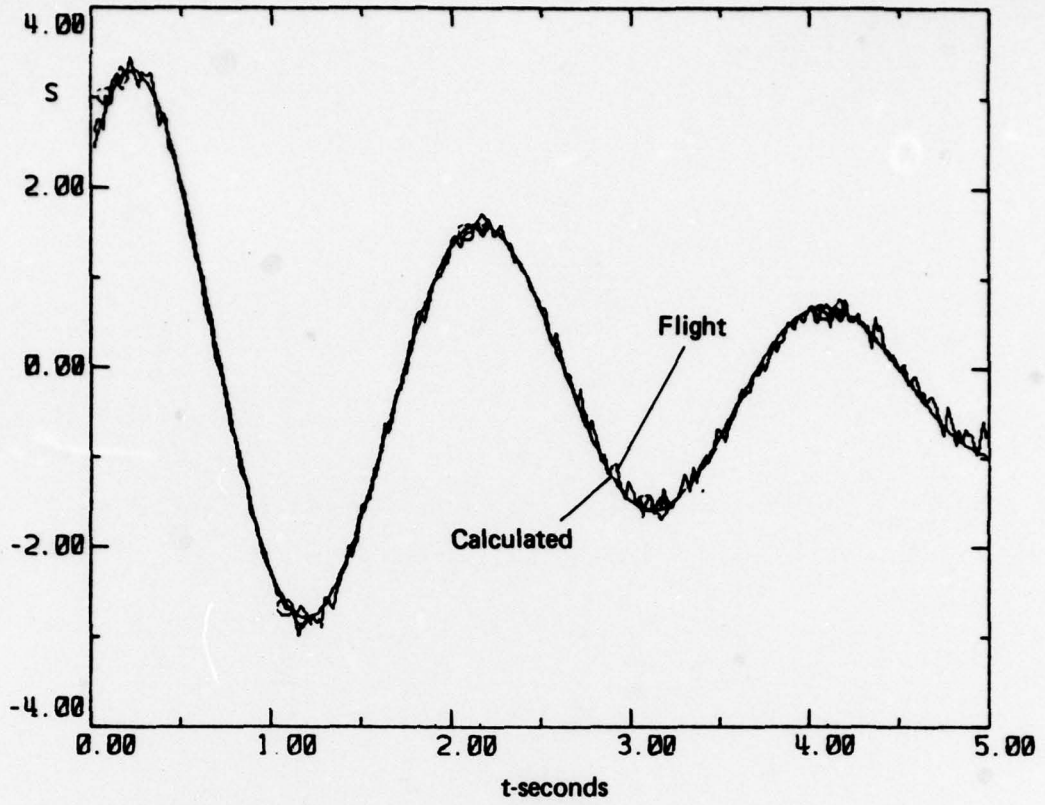

(a) Shear

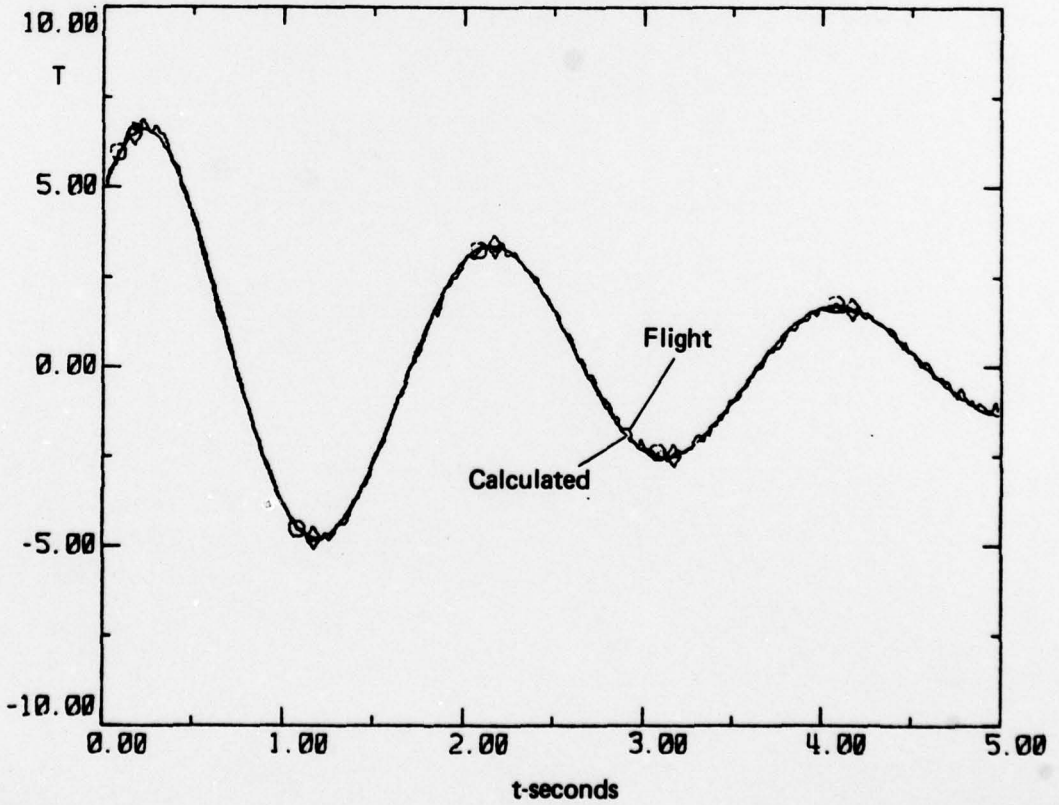

(b) Tension

FIG. 12. MATCHED FIN LOADS – RKI – 4

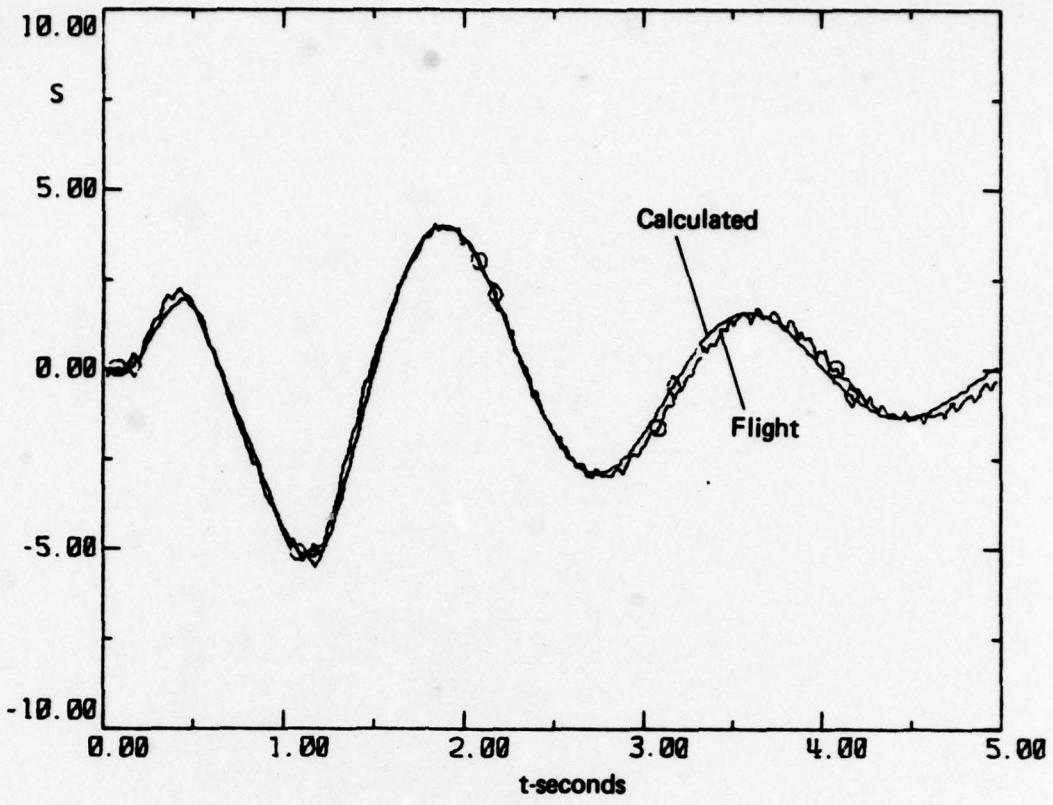

(a) Shear

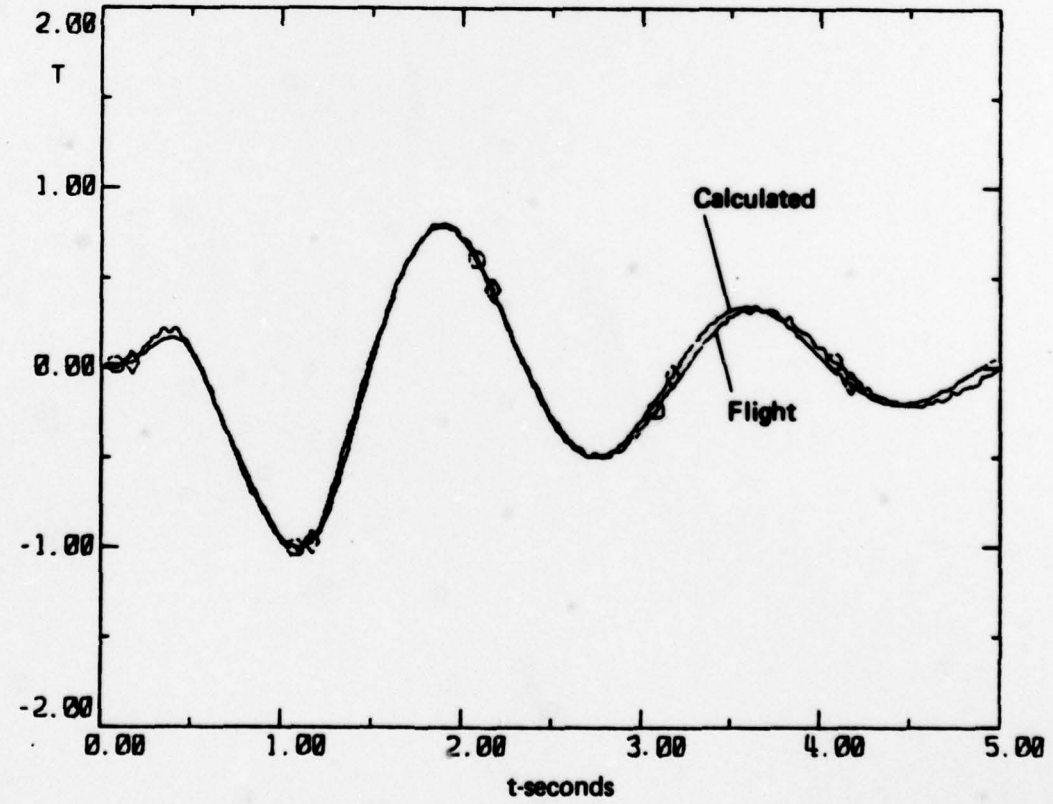

(b) Tension

FIG. 13. MATCHED FIN LOADS – RK2 – I

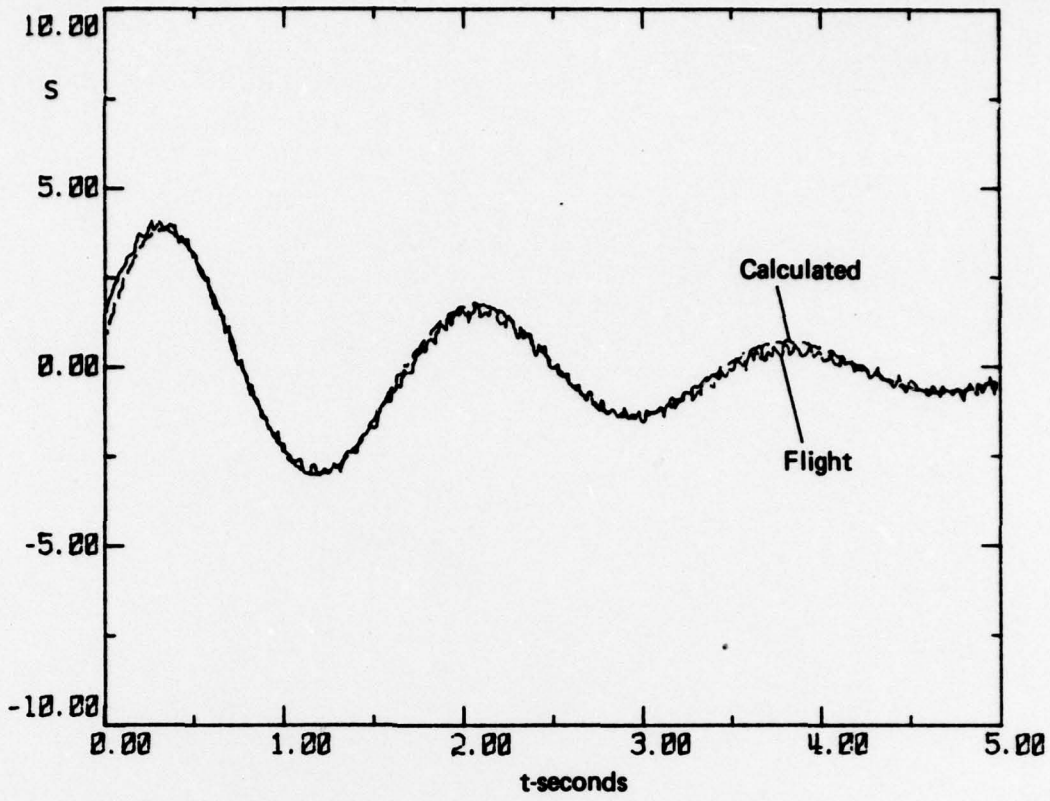

(a) Shear

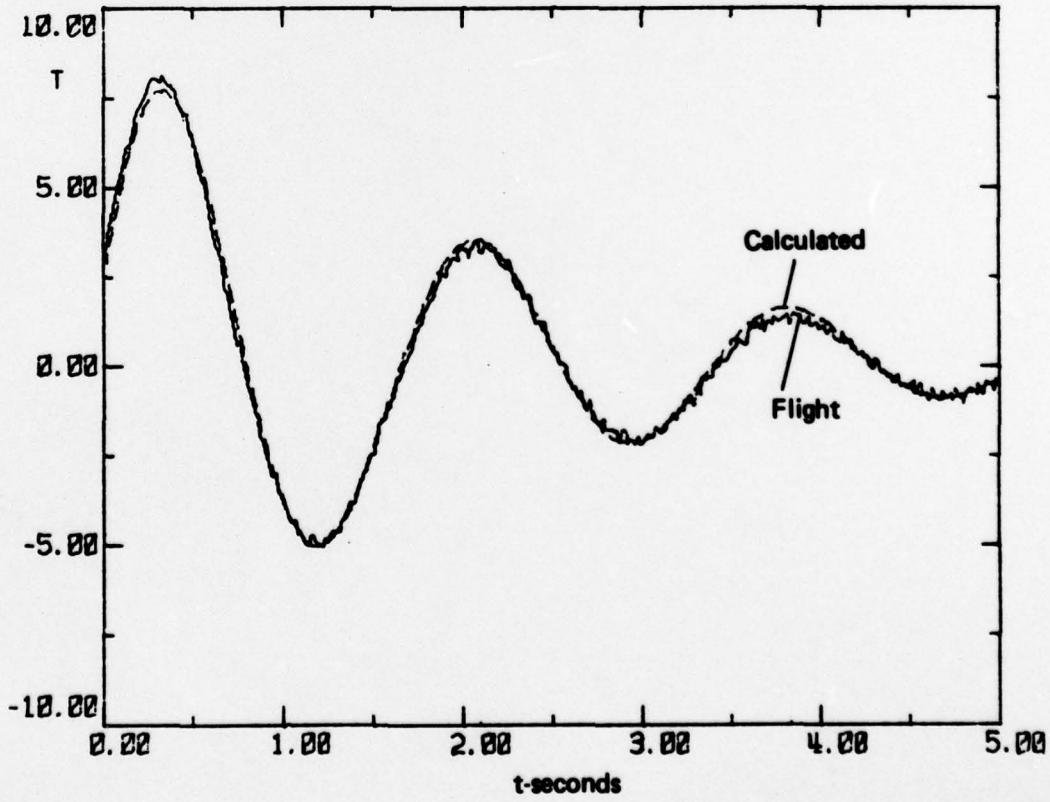

(b) Tension

FIG. 14. MATCHED FIN LOADS – RK2 – 3

DOCUMENT CONTROL DATA SHEET

Security classification of this page: Unclassified

1. Document Numbers
   (a) AR Number:
   AR-001-311
   (b) Document Series and Number:
   Aerodynamics Note 380
   (c) Report Number:
   ARL-Aero-Note-380

2. Security Classification
   (a) Complete document:
   Unclassified
   (b) Title in isolation:
   Unclassified
   (c) Summary in isolation:
   Unclassified

3. Title: LATERAL AERODYNAMICS EXTRACTED FROM FLIGHT TESTS USING A PARAMETER ESTIMATION METHOD

4. Personal Author(s):
   R. A. Feik

5. Document Date:
   October 1978

6. Type of Report and Period Covered:

7. Corporate Author(s):
   Aeronautical Research Laboratories

8. Reference Numbers
   (a) Task: DST 74/21
   (b) Sponsoring Agency:

9. Cost Code:
   54 7730

10. Imprint
    Aeronautical Research Laboratories,
    Melbourne

11. Computer Program(s)
    (Title(s) and language(s))

12. Release Limitations (of the document): Approved for public release

12-0. Overseas:	No.		P.R.	1	A		B		C		D		E	

13. Announcement Limitations (of the information on this page): No limitation

14. Descriptors:
    Flight Tests
    Delta Wings
    Parameter Estimation
    Newton-Raphson Method

15. Cosati Codes: 1201
    1402

16.

ABSTRACT

Flight data from a 60° delta wing aircraft have been analysed using a modified Newton-Raphson parameter estimation procedure. The model equations used for the analysis were extended to account for sideslip vane errors and for lateral accelerometer position error. Lateral derivatives extracted from the data have been compared with wind tunnel measurements and theoretical estimates and areas of agreement and disagreement identified. The method has also been applied to the analysis of fin loads measured in flight and some tentative conclusions reached. The results confirm the effectiveness of the parameter identification procedure in flight test analysis and its ready applicability to a variety of related problems.

DISTRIBUTION

	Copy No.
AUSTRALIA	
DEPARTMENT OF DEFENCE	
Central Office	
Chief Defence Scientist	1
Executive Controller, ADSS	2
Superintendent, Defence Science Administration	3
Australian Defence Scientific and Technical Representative (UK)	4
Counsellor, Defence Science (USA)	5
Defence Library	6
JIO	7
Assistant Secretary, DISB	8–23
Aeronautical Research Laboratories	
Chief Superintendent	24
Superintendent—Aerodynamics Division	25
Divisional File—Aerodynamics Division	26
Author: R. A. Feik	27
Library	28
D. A. Secomb	29
J. A. Rein	30
P. Gottleib	31
C. A. Martin	32
A. J. Farrell	33
N. E. Gilbert	34
C. R. Guy	35
D. A. Frith	36
J. B. Willis	37
C. K. Rider	38
D. A. H. Bird	39
D. C. Collis	40
Materials Research Laboratories	
Library	41
Defence Research Centre	
Library	42
Mr. R. L. Pope	43
Air Office	
Air Force Scientific Adviser	44
Aircraft Research and Development Unit (Scientific Flight Group)	45
Aircraft Research and Development Unit (Mr. G. Morgan)	46
Engineering (CAFTS) Library	47
HQ Support Command (SENGSO)	48
DEPARTMENT OF PRODUCTIVITY	
Australian Government Engine Works	
Mr. J. L. Kerin	49